MEDWIN PUBLISHERS
Committed to Create Value for Researchers

Food Science & Nutrition Technology
ISSN: 2574-2701

Supplementary Material

Supplementary data D1: Raw data files of instrumentations

https://drive.google.com/open?id=1B6zdojSaeMMYSHXS0mWuRKhwyGnbZZ0L

Supplementary video V1: Method of MIRGA spraying

https://drive.google.com/open?id=1QoRwTESKfSdoJTfD--xIG9YpTDnVonGW

Supplementary figure F1: MIRGA spray diagram

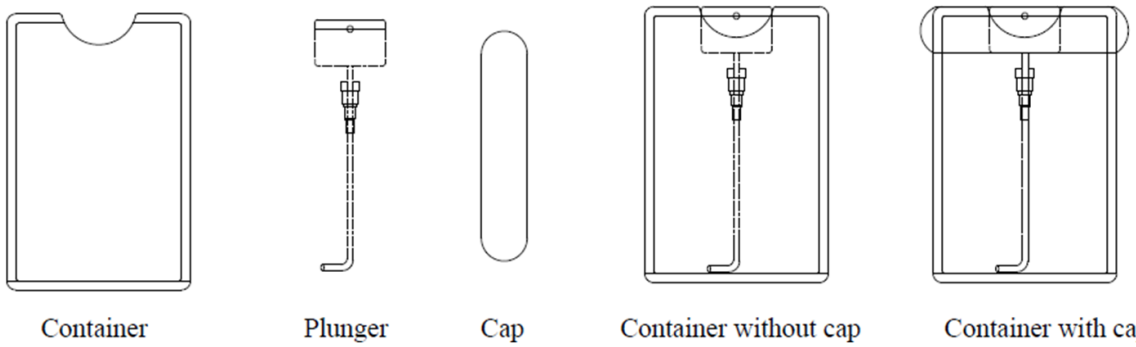

Figure 1: MIRGA spray diagram.

Supplementary Text T1: Details of MIRGA

MIRGA (patent no.: 401387) is a 20-mL capacity polypropylene plastic atomizer containing an inorganic (molar mass 118.44 g/mole) water-based solution in which approximately two sextillion cations and three sextillion anions are contained. The sprayer unit has dimensions 86 × 55 × 11 mm, an orifice diameter of 0.375 mm, ejection volume 0.062 + 0.005 mL, and ejection time 0.2 s. The average pressure is 3900 Pa, and the cone liquid back pressure is 2000 N/m2 (Supplementary Fig (ii)). During spraying, approximately 1-µg weight of water is lost as mist and the non-volatile material in the sprayed liquid has a concentration of 153 mg/mL. Every time spraying emits 0.06ml which contains approximately seven quintillion cations and eleven quintillion anions.

Depending on the pressure applied to the plunger, every spraying is designed to generate 2–6 µm as estimated by an FTIR (retro-reflector) interferometer instrument (Detector type D* [cm HZ1/21] MCT [2-TE cooled]) at Lightwind, Petaluma, CA, USA.

Text T2: Detailed Discussion

Detailed Discussion [1]

Invention Background: The four observable states of matter (solid, liquid, gas, and plasma) are composed of intermolecular and intermolecular bonds. The inherent characteristics of neutrons, protons and electrons are unique, however, differences in their numbers are what constitute different atoms, and how these atoms bind together develops into different molecules with unique characteristics. In the electromagnetic wave (EMW) spectrum, the mid-IR region is vital and interesting for many applications since this region coincides with the internal vibration of most molecules [2]. Almost all thermal radiation on the surface of the Earth lies in the mid-IR region, indeed, 66% of the Sun's energy we receive is infrared [3] and is absorbed and radiated by all particles on the Earth. At the molecular level, the interaction of mid-IR wavelength energy elicits rotational and

vibrational modes (from about 4500–500 cm-1, roughly 2.2 to 20 microns) through a change in the dipole movement, leading to chemical bond alterations [4]. During our research we have observed: (A) In all objects, even though atoms always remain as atoms, their chemical bond parameters are continuously prone to alteration by cosmic and physical energies (e.g.: EMW, heat, pressure, and humidity) causing the bonds to compress/stretch/bend [4-7], break [8,9], or new bonds to be formed [10]. These alterations ultimately lead to changes in the physicochemical characteristics of the objects. (B) The dynamic, constant, and mutual influences of EMW among the Earth and the celestial and living bodies are continuously causing alterations in the inherent physiochemical characters of earthly objects, for instance, enhancement due to an optimum dose of energy or decrease/destruction due to a high dose of energy (detailed below). Thus, based on these concepts, MIRGA was developed to alter the bond parameters, thereby potentiating the natural characteristics of products.

MIRGA Definition: We define MIRGA as 'a harmless, economical atomizer containing an imbalanced ratio of ions suspended in water, which influence the natural potency of target substances by generating mid- IR while spraying'.

Technique of Mid-IR Generation from MIRGA: We designed MIRGA as to accommodate an imbalanced ratio of ions suspended in water in their fundamental state, which can move as free particles. The solution exhibits very little detectable background frequency, below even that of cosmic events. By comparison humans emit more radioactivity (around 10 microns) [11,12]. We designed MIRGA to generate energy based on various processes such as:(A) spraying leads to ionization (electrons getting separated from atoms) and many pathways for electron re-absorption; due to these two oscillatory processes, energy is generated;(B) while spraying, a water-based ionic solution gets excited/charged, which in turn leads to oscillation among the imbalanced ions [13] in their excited state, resulting in the emission of photons [14,15]; (C)although a low electromagnetic field exists between the charged particles of the MIRGA's ionic solution, during spraying the induced oscillation between these charged particles produces energy [16-20]; and(D) in the natural rainfall process, more energy is required to break the water bonds for creating smaller water droplets [21]. Therefore, these droplets should have more stored energy, which then travels down at velocity from a specific distance, thus gaining kinetic energy. When the rain hits the Earth's surface, it forms a very thin film of mid-IR (nearly 6 micron), hence there is a net heat gain [21,22]. We simulated this rainfall's energy-gaining process in MIRGA(i.e., when imbalanced ions in liquid media are atomized, the ejected smaller droplets should have higher internal energy as well as acquired kinetic energy, and the energy emitted by breaking the surface tension). From trial and error, we calibrated the ejection pressure to obtain a desired fine mist, and minimized the evaporation rate by altering the pH and density of the solution. Moreover, the accelerated ions in the sprayed ionic clouds collide among themselves and generate energy [23], thus, we incorporated these phenomena in our atomizer and designed it in such a way as to emit energy in the 2–6 μm mid- IR depending on the given plunger pressure. Yousif, et al. [24] described this process as a photodissociation of molecules caused by the absorption of photons from sunlight, including those of infrared radiation, visible light, and ultraviolet light, leading to changes in the molecular structure.

Safety of MIRGA-Sprayed Products: In our nearly two-decades of research, we have observed that MIRGA-induced bond-altered target substances do not show any adverse reaction upon consumption/use. In nature, (A) Stereochemical configuration has great influence on taste [25] (e.g., varieties of mango, grapes, rice, etc.), (B) Cooking and digestive enzymes break chemical bonds, thereby softening foods. This indicates that alterations in chemical bonds occur naturally and do not represent a risk to human health. As an example, boiled rice, puffed rice, flat rice, and rice flour have a unique aroma, taste, texture, and shelf-life but conserving the same molecular formula ($C_6H_{10}O_5$). (C) In the food industry, sensory attributes and shelf-life are enhanced by altering the food's chemical bonds using various irradiation processes like radappertization, radicidation, and radurization [26]. (D) Upon heating, water changes from ice to liquid to steam, which are manifestations of changes in the hydrogen bonds [27] but the chemical composition (H_2O) remains the same [28].

MIRGA's Primeval and Future Scope: The water-based MIRGA could be the first novel potentiating technology. This type of atomizer technology also seems to be present with the extra-terrestrials for their therapeutic use during visitations [29]. In various products, we have achieved a range from 30% to 173% potentiation. Even the smaller improvement resulted in 30% monetary and resource savings as well as health benefits. However, there is a knowledge gap between potentiation from 30% to at least 100% for all products, which can be filled-up by refining MIRGA's ionic solution, concentration, atomizer pressure, and other parameters and even formulating a better solution. Various mid-IR emitters are now available (e.g., silicon photonic devices [30], cascade lasers quantum and interband [31], non-cascade-based lasers, chalcogenide fiber-based photonic devices [32], and suspended-core tellurium-based chalcogenide fiber photonic devices) [33]. These emitters are not as cost-effective as MIRGA and are useful only in astronomy, military, medicine, industry, and research applications. These emitters are too complex for domestic application by the average user. Because of MIRGA's wide range of applications, we believe that this technique will

resonate in many scientific fields including biophotonics, therapeutics, health, ecology, and others. We are currently conducting research on MIRGA and its applications, namely MIRGA salt, MIRGA vapor and MIRGA plasma.

References

1. Umakanthan T, Mathi M, 2022. Decaffeination and improvement of taste, flavor and health safety of coffee and tea using mid-infrared wavelength rays. Heliyon 8(11): e11338.
2. CORDIS European commission (2015) New advances in mid-infrared laser technology, Compact, high-energy, and wavelength-diverse coherent mid-infrared source.
3. Aboud SA, Altemimi AB, Al-Hilphy ARS, Yi-Chen L, Cacciola F (2019) Molecules A Comprehensive Review on Infrared Heating Applications in Food Processing. Molecules 24(22): 4125.
4. Girard JE (2014) Principles of Environmental Chemistry, 3rd(Edn.), Jones & Bartlett Learning, USA, pp: 99.
5. Alvarez-Ordóñez A, Prieto M (2012) Fourier Transform Infrared spectroscopy in Food Microbiology, Springer Science & Business Media, pp: 3.
6. Smith BC (1998) Infrared Spectral Interpretation: A Systematic Approach, CRC Press, LLC, pp :7.
7. Shankar DR (2017) Remote Sensing of Soils. Germany: Springer-Verlag GmbH, pp: 268.
8. Mohan J (2007) Organic Spectroscopy: Principles and Applications, 2nd(Edn.), Alpha Science International, Harrow, UK.
9. McMakin C (2011) Frequency specific Microcurrent in pain management E-book, Elsevier, China, pp: 30.
10. Williams G, Moss D, Barnett NW (2011) Biomedical Applications of Synchrotron Infrared Microspectroscopy: A Practical Approach, Royal Society of Chemistry, UK, pp: 58.
11. Raven PH, Berg LR, Hassenzahl DM (2012) Environment, John Wiley & Sons, USA, pp: 45.
12. Ashcroft F (2000) Life at the Extremes: The Science of Survival, University of California Press, California, pp: 122.
13. Sanders RH (2014) Revealing the Heart of the Galaxy, Cambridge University Press, USA, pp: 70.
14. Verheest F (2000) Waves in Dusty Space Plasmas, Kluwer Academic Press, Dordrecht, pp: 89.
15. Sun Keping, Yu G (2004) Recent developments in Applied Electrostatics. Proceedings of the Fifth International Conference on Applied Electrostatics, Elsevier, China, pp: 87.
16. Fauchais PL, Heberlein JVR, Boulos MI (2014) Thermal Spray Fundamentals From Powder to Part. Springer Science & Business Media, New York, pp: 84.
17. Wendish M, Brenguier JL (2013) Airborne Measurements for environmental Research: Methods and Instruments, Wiley-VCH, pp: 641.
18. Singh KC (2009) Basic Physics, PHL Learning Private Limited, New Delhi, pp: 413.
19. Prasad M (2017) Soul, God and Buddha in Language of Science, Notion Press, Chennai, pp: 608.
20. Stephen Pople (1999) Complete Physics, Oxford University Press, Oxford, pp: 166.
21. Barry RG, Chorley RJ (1998) Atmosphere, Weather and Climate, 7th(Edn.), Routledge, London, pp: 51.
22. (1995) Eniday
23. Krishnakumar T (2019) Application Of Microwave Heating In Food Industry, pp: 1-19.
24. Yousif E, Haddad R (2013) Photodegradation and photostabilization of polymers, especially polystyrene: review. SpringerPlus

2: 398.

25. Williamson KL, Masters KM (2011) Macroscale and Microscale Organic Experiments, 6th(Edn.), Brooks/ Cole C engage learning, CA, pp: 720.

26. Sivasankar B (2014) Food Processing and preservation, PHI Learning Private Limited, Delhi, pp: 246.

27. Trevor Day (1999) Ecosystems: Oceans. Routledge Taylor & Francis Group, London and New York, pp: 44.

28. Raymond KW (2010) General Organic and Biological Chemistry, 3rd (Edn.), John Wiley & Sons, USA, pp: 176.

29. Blue planet project: Alien Technical research–25, Westchester Camp, Office of the Central Research #3, pp: 80-81.

30. (2012) CMOS Emerging Technologies. CMOSET, pp: 49.

31. Jung D, Bank S, Lee ML, Wasserman D (2017) Next-generation mid-infrared sources. Journal of Optics, 19(12): 123001.

32. Sincore A, Cook J, Tan F, El Halawany A, Riggins A, et al. (2018) High power single- mode delivery of mid-infrared sources through chalcogenide fiber. Optics Express 26(6): 7313-7323.

33. Wu B, Zhao Z, Wang X, Tian Y, Mi N, et al. (2018) Mid-infrared supercontinuum generation in a suspended-core tellurium-based chalcogenide fiber. Optical Materials Express 8(5): 1341-1348.

Instrument Details

Chemical compound transformation – GCMS, HPLC Chemical bond changes – FTIR
Structural changes – PXRD Proton resonances – Proton NMR Configuration – HR-TEM
Contour and signal-to-noise ratio – 3D Fluorescence spectroscopy Minerals estimation – ICP-AES

Pepper

HPLC: Flexar Quaternary Pump - FXQPump-1.
GCMS: Agilent technologies, 7820 GC system, 5977E MSD, Colomn DB-5, Over temp 100- 2700C, Detector MS, Flow rate 1.2, Carrier gas Helium.
FTIR: JASCO FT-IR 4200 plus spectrophotometer with ATR (range 4000–400 cm^{-1} at 298 K).
PXRD: XRD Diffractometer (powder) Philips Xpert MPD Range (2θ): 3º to 136º; X-ray tube: Cu; JCPDF database; 2θ vs intensity plots/X-ray diffractograms. Source: Cu target X-Ray tube. X-Ray Power: 2KW. Detector: Xe-filled Counterate or Proportional detector. Software: JCPDF database for powder diffractometry. Goniometer. Operation Modes: Vertical & Horizontal. Accuracy: ±0.0025. 2º θMeasurement range: 30 to 136º. Diffractometer radius: 130 to 230 m.
HR-TEM: JEOL JEM2100 PLUS; HT: 60-200Kv; Source: LAB-6 Filament; Point-point resolution: 0.23 nm; Line resolution: 0.14 nm. Model: Cryoplunge 3 system Model 930 & Elsa Cryo-Transfer Holder Model 698).
1H-NMR: The 1H NMR spectra of the compounds were performed on a 500 MHz Bruker AVANCE III spectrometer operating at 500.13 MHz , using a 5-mm broad band (BBO) probe equipped with a z-gradient coil (Bruker-Biospin, Switzerland). The samples were dissolved in CDCl 3. The chemical shifts (δ) were calibrated with reference to TMS. All 1D spectra were acquired with 32K data points. Typical acquisition parameters for the 1 H NMR experiments were as follows: acquisition time 1.58 s, spectral width 10330 Hz, pulse width 3.5 μs (flip angle ≈30 ◦), relaxation delay 1s and number of scans 32.
3D Fluorescence Spectroscopy: 3D Fluorescence spectra were measured on a Hitachi F-7000 spectrophotometer in the range of 200-700 nm (fluorescence) at 298 K. The spectral patterns were analyzed using an original software (Hitachi).

Chili Pepper

GCMS: Agilent technologies, 7820 GC system, 5977E MSD, Colomn DB-5, Over temp 100- 2700C, Detector MS, Flow rate 1.2, Carrier gas Helium.
FTIR: JASCO FT-IR 4200 plus spectrophotometer with ATR (range 4000–400 cm^{-1} at 298 K)
HR-TEM: JEOL JEM2100 PLUS; HT: 60-200Kv; Source: LAB-6 Filament; Point-point resolution: 0.23 nm; Line resolution: 0.14 nm. Model: Cryoplunge 3 system Model 930 & Elsa Cryo-Transfer Holder Model 698)
1H-NMR: The 1H NMR spectra of the compounds were performed on a 500 MHz Bruker AVANCE III spectrometer operating at

500.13 MHz , using a 5-mm broad band (BBO) probe equipped with a z-gradient coil (Bruker-Biospin, Switzerland). The samples were dissolved in CDCl 3. The chemical shifts (δ) were calibrated with reference to TMS. All 1D spectra were acquired with 32K data points. Typical acquisition parameters for the 1 H NMR experiments were as follows: acquisition time 1.58 s, spectral width 10330 Hz, pulse width 3.5 μs (flip angle ≈30 ◦), relaxation delay 1s and number of scans 32.

3D Fluorescence spectroscopy: 3D Fluorescence spectra were measured on a Hitachi F-7000 spectrophotometer in the range of 200-700 nm (fluorescence) at 298 K. The spectral patterns were analyzed using an original software (Hitachi).

Ginger

GCMS: Agilent technologies, 7820 GC system, 5977E MSD, Colomn DB-5, Over temp 100- 2700C, Detector MS, Flow rate 1.2, Carrier gas Helium.

FTIR: JASCO FT-IR 4200 plus spectrophotometer with ATR (range 4000–400 cm^{-1} at 298 K)

PXRD: Rigaku RINT 2500 X-ray diffractometer (CuKα anode; λ = 1.541 Ao). Samples scanned at 40kV and 30mA from 50 to 350 2θ values and analyzed using a PDXL2 software (Rigaku).

HR-TEM: FEI Technai Spirit G2, HT 120KV, Electron source LaB6, Netherlands.

1H-NMR: The 1H NMR spectra of the compounds were performed on a 500 MHz Bruker AVANCE III spectrometer operating at 500.13 MHz , using a 5-mm broad band (BBO) probe equipped with a z-gradient coil (Bruker-Biospin, Switzerland). The samples were dissolved in CDCl 3. The chemical shifts (δ) were calibrated with reference to TMS. All 1D spectra were acquired with 32K data points. Typical acquisition parameters for the 1 H NMR experiments were as follows: acquisition time 1.58 s, spectral width 10330 Hz, pulse width 3.5 μs (flip angle ≈30 ◦), relaxation delay 1s and number of scans 32.

Curry Leaves

GCMS: Agilent technologies, 7820 GC system, 5977E MSD, Colomn DB-5, Over temp 100- 2700C, Detector MS, Flow rate 1.2, Carrier gas Helium.

FT-IR: A small quantity of the sample is added to KBr in the ratio 1:100 approximately. The matrix is grind for 3-4 minutes using mortar and pestle. The fine powder is transferred into 13 mm diameter die and made into a pellet using a hydraulic press by applying a pressure of 7 tonnes. The fine pellet is subjected to FTIR analysis using universal pellet holder. (a single drop of oil is poured on the KBr pellet in case of liquid samples). Infrared spectral data were collected on Thermo Avtar 370 FTIR spectrometer Spectra are collected over a range of 4000– 400 cm−1at 4 cm−1 resolution with an interferogram of 32 scans.

PXRD: The sample is smeared over low back ground sample holder (amorphous silica holder) and fixed on the sample stage in goniometer. The instrument is set with B-B geometry. The current and voltage is set to 40 mV and 35 mA and data has been collected. Instrument make: Bruker Model D8 Advance Goniometer: theta/2 theta.

TEM: An extremely small amount of material is suspended in water/ethanol (just enough to obtain slightly turbid solution). The solution is homogenised using ultrasonicator to disperse the particles, a drop of the solution is then pippeted out and cast the drop on carbon-coated grids of 200 mesh the grid is dried and fixed in the specimen holder. Instrument Make: Jeol Model JM 2100.

1H-NMR: The experiments were done on a 600 MHz NMR SPECTROMETER (ECZR Series, JEOL, JAPAN) using a 3.2mm CPMAS probe at 150MHz frequency. All the samples were run at 18KHz spinning speed at Room Temp and with a delay of 5sec.

Fenugreek, Cumin, Corainder

GCMS: Gas Chromatogram Mass Spectrometer Shimadzu GC-QP2010S.

FTIR: Make: JASCO, Model: FTIR/4200. Resolution: 2 cm-1. Scan: 60 sec. Range: 400-4000 Cm-1. Software: JASCO Spectra Manager for spectra Analysis.

PXRD: Make: Rigaku Model: (Ultimata IV). CuKα anode; λ = 1.541 Ao).Each sample was consolidated in an Quartz glass holder and scanned at 40kV and 30mA from 5 o to 50 2θ values using a scanning period of 2 deg/min and a step size of 0.02 . The powder diffraction patterns were analyzed using PXDL software and plotted using OriginPro 7.5.

TEM: FEI Technai Spirit G2, HT 120KV, Electron source LaB6, Netherlands.

13C Solid State NMR: The experiments were done on a 600 MHz NMR SPECTROMETER (ECZR Series, JEOL, JAPAN) using a 3.2mm CPMAS probe at 150MHz frequency. All the samples were run at 18KHz spinning speed at Room Temp and with a delay of 5sec.

Black Cumin, Cardamom

GCMS: Agilent technologies, 7820 GC system, 5977E MSD, Colomn DB-5, Over temp 100- 2700C, Detector MS, Flow rate 1.2, Carrier gas Helium.
FTIR: IR AFFINITY I – FTIR Spectrophotometer, FTIR 7600, Shimadzu.
PXRD: The sample is smeared over low back ground sample holder (amorphous silica holder) and fixed on the sample stage in goniometer. The instrument is set with B-B geometry. The current and voltage is set to 40 mV and 35 mA and data has been collected. Instrument make: Bruker Model D8 Advance Goniometer: theta/2 theta.
TEM: An extremely small amount of material is suspended in water/ethanol (just enough to obtain slightly turbid solution). The solution is homogenised using ultrasonicator to disperse the particles, a drop of the solution is then pippeted out and cast the drop on carbon-coated grids of 200 mesh the grid is dried and fixed in the specimen holder. Instrument Make: Jeol Model JM 2100.
1H-NMR: The 1H NMR spectra of the compounds were performed on a 500 MHz Bruker AVANCE III spectrometer operating at 500.13 MHz , using a 5-mm broad band (BBO) probe equipped with a z-gradient coil (Bruker-Biospin, Switzerland). The samples were dissolved in CDCl 3. The chemical shifts (δ) were calibrated with reference to TMS. All 1D spectra were acquired with 32K data points. Typical acquisition parameters for the 1 H NMR experiments were as follows: acquisition time 1.58 s, spectral width 10330 Hz, pulse width 3.5 μs (flip angle ≈30 ◦), relaxation delay 1s and number of scans 32.
ICP-AES (only for Black cumin) (Inductively Coupled Plasma-Atomic Emission Spectroscopy): Make: SPECTRO Analytical Instruments GmbH, Germany; Model: ARCOS, Simultaneous ICP Spectrometer.

Detailed Instrumentation Analysis:

GCMS Instrumentations

Pepper: The two main peaks appearing in all samples were due to Caryophyllene and Peperine at 6.08 min and 20.36 min, respectively. Both compounds are commonly found in black pepper. Caryophyllene is known to contribute to the aroma of black pepper, while Peperine contributes to the hotness and pungency. Table shows the changes to the peak area of these compounds between the control and 2 and 10 sprayed samples. Despite the significant rise in the level of Peperine in 10 sprayed sample by almost 50%, there was a downgrade for the quality (reduction in both hotness and aroma) of this sample, compared to a control or 2 sprayed sample. This may be attributed to the formation of other degradation products due to 10 spraying which are structurally related to fatty acids, such as the compounds appearing as peaks at 11.36 min and 13.0 min. It seems that the three samples contain mostly piperine and according to sample information, the hotness reduced on 10 sprayed sample, is the result on the changes on piperine isomer configuration.

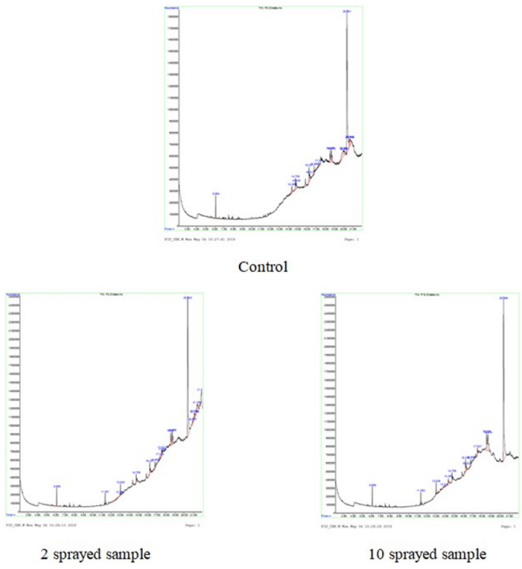

Figure 2: GCMS – Pepper.

Rt (min)	Name of compound	% Area present in each sample			Remarks
		Control	2 sprayed	10 sprayed	
6.08	Caryophylene	3.35	3.17	2.95	Spectrum very similar to reported
11.36	Hexadecanoic acid methyl ester	0	2.05	1.95	Spectrum very similar to reported
13.03	Octadecenoic (Z)- methyl ester	0	2.32	1.91	Commonly found on cloves
14.36	(Z)-6-octadecenoic acid	3.22	Not integrated	0.58	Probably oleic acid isomer
14.75	Oleic acid	2.92	1.13	1.63	Omega 9 oil type, present in seeds
14.84	E-9-octadecenoic acid	2.5	0	0	Probably oleic acid isomer
16.21	2-methyl-ZZ-3, 13 octadienol	4.2	2.24	3.88	
16.31	2,3-Dihydroxypropyl elaidate	2.46	Not integrated	1.43	
16.8	Long chain acid ester	1.74	1.8	2.18	m/z = 207 and m/z= 149 from column bleeding and plasctizicers phtalates
17.31	Long chain acid ester	0.88	1.01	Not integrated	m/z = 207 and m/z= 149 from column bleeding and plasticizers phthalates
18.53	Possible column bleeding	3.64	4.66	6.59	
18.67	Possible column bleeding	4.31	5.45	11.13	
20.36	Piperine	54.44	58.71	62.59	Most Abundant peak in all samples

Table 1: GCMS – Pepper.

Chili Pepper:

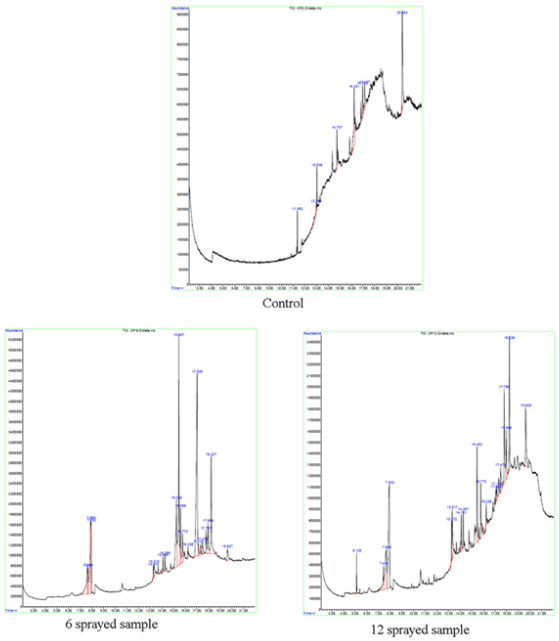

Figure 3: GCMS – Chilli Pepper.

Rt (min)	Name of compound	% Area present in each sample			Remarks
		Control	6 sprayed	12 sprayed	
11.36	Hexadecanoic acid, methyl ester	11.37	ND	ND	Long chain acid ester
13.03	8-Octadecenoic acid, methyl ester	6.34	ND	ND	Long chain acid ester
14.75	cis-Vaccenic acid	5.49	ND	ND	
15.47	Long chain saturated molecule	ND	17.2	6.69	Probably capsaicin analogue
16.23	12-Octadecenoic acid, methyl ester	23.4	ND	0.5	Long chain acid ester
16.91	2,3-Dihydroxypropyl elaidate	8.74	ND	ND	
17.02	Long chain saturated molecule	ND	26.52	ND	Probably capsaicin analogue
17.96	Long chain saturated molecule	ND	2.6	4.39	Probaly capsaicin
18.22	Long chain saturated molecule	ND	8.84	10.67	Probably capsaicin analogue
19.62	9-Octadecenoic acid (Z)-, 2-hydr…	ND	1.49	8.2	
20.36	Piperine	34.94	ND	ND	Most Abundant peak in control sample

Table 2: GCMS – Chilli Pepper.

- **Spectra Analysis and Conclusion**

The next structure shows main fragments that should appear on capsaicin spectrum.

Control sample contains as main component piperine and very small amounts of other compounds such as long chain acid esters commonly found on seeds (octadecenoic and hexadecanoic acids esters). 6 and 12 sprayed samples show peaks on 7.4 min -8 min which do not correspond to molecules commonly found on foods, this compounds may come from sample containers. Two of the treated samples 6 and 12 sprayed samples show peaks at the retention times 15.47 min and 17.02 min, these peaks could be related to the hotness of the sample, since this sample spectra appear to be capsaicinoid molecules. If we analyse specifically peaks on 15.47 min and 17.02 min, both peaks disappear on 12 sprayed sample which could explain hotness reduction on 12 sprayed sample. In conclusion sample sprayed 6 times shows new compounds which again disappear on the sample that was sprayed 12 times. This compounds structures may be related to capsaicin analogues. Below appears on figures 2 and 3 a comparison of capsaicin reported spectra with samples spectra.

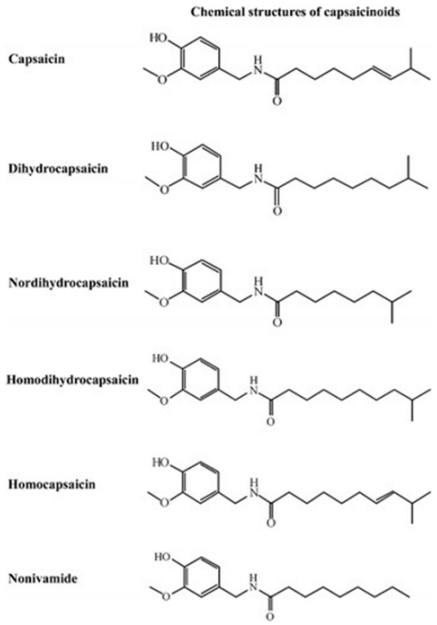

Figure 4: Capsaicin analogues that contribute to hotness on pepper.

Most capsaicin analogues show very similar fragmentation on electronic impact mass spectrometry.
Recommendation: Acquire spectra with lower ionization energy or adjust instrumental parameters to see higher mass fragments.

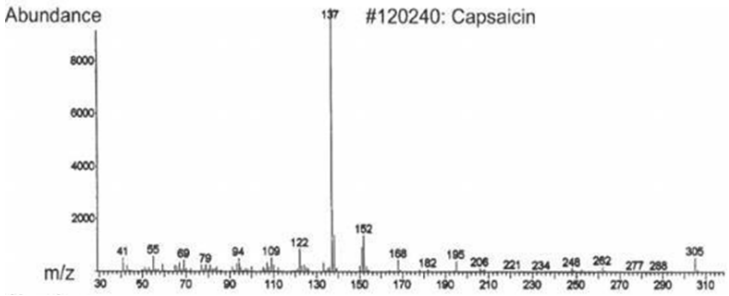

Figure 5: Capsaicin reported spectrum.

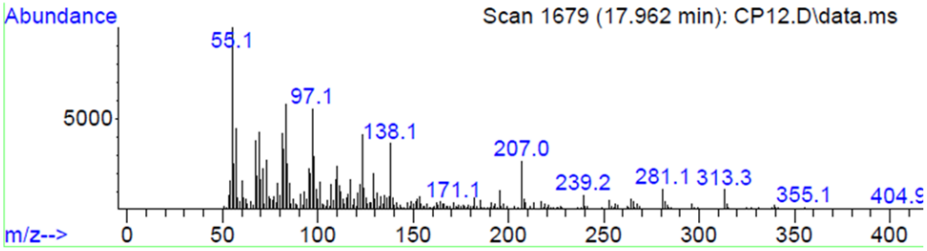

Figure 6: spectra from 17.96 peak on sample CP12.

Figures 5 and 6 show a comparison of capsaicin spectrum with the spectrum extracted from 17.96 peak, this peak is the only peak that shows more similarity to capsaicin spectrum.

Ginger: Control sample contains Butan-2-one, 4-(3-hydroxy-2-methoxyphenyl)-, Di-epi-α-cedrene,)-, Fumaric acid, myrtenyl octyl ester, 17-Octadecynoic acid, 12-Methyl-E,E-2,13-octadecadien-1- ol etc. After 2 spraying, there are new unique peaks of Butan-2-one, 4-(3-hydroxy-2- methoxyphenyl), 2--Butanone, 4-(4-hydroxy-3-methoxyphenyl), Gingerol compared to control. After 8 spraying, there are unique new peaks of Cubanol, Spiro[4.5] decan-7-one, 1,8-dimethyl- 8,9-epoxy-4-isopropyl and 2,6-Dimethyl-1,3,5,7-octatetraene, E,E. While 10 spraying gives unique peaks of 1,3-Cyclohexadiene, 5-(1,5-dimethyl-4-hexenyl)-2- methyl-, [S-(R*,S*)], 2-Naphthalenemethanol, 1,2,3,4,4a,5,6,8a-octahydro-α,α,4a,8-tetramethyl-, (2α,4aα,8aα), Butan-2-one, 4-(3-hydroxy-2-methoxyphenyl), N-(3-Fluorophenyl)-2- (furfurylidenehydrazino)-2-oxoacetamide and 2-Ethyl-6-methyl-6,7-dihydro-9H-5-oxa-9- azabenzocyclohepten-8-one.

Rt (Min)	Name Of Compound	% Area Present In Each Sample				Remarks
		Control	2 sprayed	8 sprayed	10 sprayed	
24.609	1,3-Cyclohexadiene, 5-(1,5- dimethyl-4-hexenyl)-2-methyl-, [S-(R*,S*)]	0	0	0	2.2	
25.295	Di-epi-α-cedrene	2.7	1	2.7	0	
27.694	Butan-2-one, 4-(3-hydroxy-2-methoxyphenyl)	0	3.3	0	0	
28.178	Cubanol	0	0	1	0	
28.409	2-Naphthalenemethanol, 1,2,3,4,4a,5,6,8a-octahydro- α,α,4a,8-tetramethyl-, (2α,4aα,8aα)	0	0	0	1.4	

28.849	2--Butanone, 4-(4-hydroxy-3-methoxyphenyl)-	0	1	0	0	
29.188	Butan-2-one, 4-(3-hydroxy-2-methoxyphenyl)-	0	0	0	2.7	
30.197	Butan-2-one, 4-(3-hydroxy-2-methoxyphenyl)-	6.1	0	4.1	0	
34.0355	Spiro[4.5]decan-7-one, 1,8- dimethyl-8,9-epoxy-4- isopropyl.	0	0	1.7	0	
34.798	Fumaric acid, myrtenyl octyl ester	1.2	0	0	0	
34.798	2,6-Dimethyl-1,3,5,7-octatetraene, E,E.	0	0	1.8	0	
36.998	17-Octadecynoic acid	9.1	0	0	0	
37.556	N-(3-Fluorophenyl)-2- (furfurylidenehydrazino)-2-oxoacetamide	0	0	0	4	
37.724	Cyclohexanone, 2-(2-nitro-2-propenyl)	0	4	2.4	0	
38.605	12-Methyl-E,E-2,13-octadecadien-1-ol	7.3	0	0	0	
39.667	Gingerol	0	12.1	0	0	
39.957	(2,6,6-Trimethylcyclohex-1-enylmethanesulfonyl) benzene	10.9	0	23.1	0	
40.942	Gingerol	31	50	31.6	57.5	Highest in 2 and 10 sprayed sample
41.896	1-Hexadecanol, 2-methyl	2.9	0	0	0	
43.551	Naphthalene, 1-(1- decylundecyl) decahydro-	2.7	0	0	0	
44.414	Gingerol	12.8	10.8	11.1	12.9	
48.624	2-Ethyl-6-methyl-6,7-dihydro- 9H-5-oxa-9-azabenzocyclohepten-8-one	0	0	0	4	
50.348	9-Octadecenamide, (Z)-	10.9	14.5	13.9	8.9	

Table 3: GCMS – Ginger.

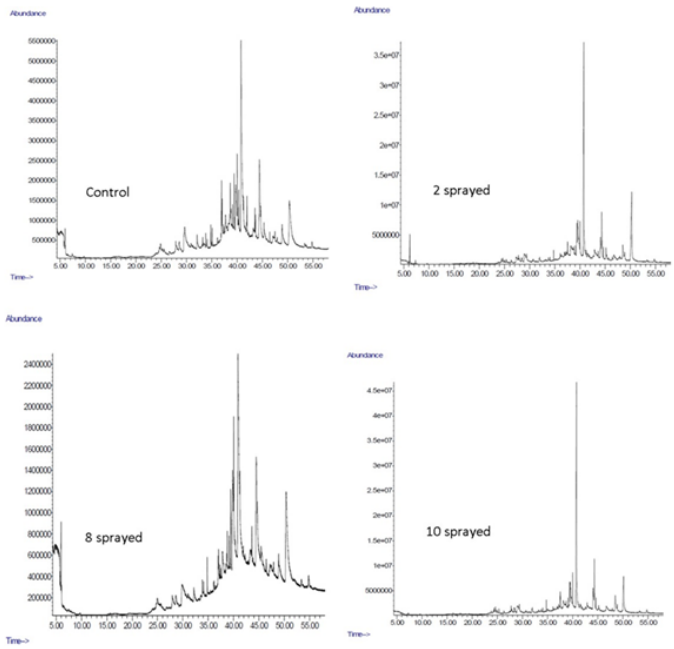

Figure 7: GCMS – Ginger.

Fenugreek: After 2 spraying, there was new peak of Hygrine & traces of Palmitic acid. This might be responsible for reduction in bitterness. While 6 sprayed sample has shown unique peak of Krypton with increase in oleic acid, this might be responsible for further loss in bitter taste and a stringency.

R.T.(Min)	Name of Compound	% Area Present in each sample			Remarks
		Control	2 sprayed	6 sprayed	
1.065	1-Hexacosene	1.95	3.76	4.33	
1.709	Trichloromethane-(chloroform)	37.5	14.61	33.3	2 spraying detoxified the chloroform
1.656	4H-1,2,4-Triazol-4-amine	0	0	20.19	Most abundant peak in 6 sprayed sample
1.789	4H-1,2,4-Triazol-4-amine	0	0	11.59	
1.816	Krypton	0	0	29.91	Most abundant peak in 6 sprayed sample
1.956	Methane-d, trichloro	60.53	41.95	0	
1.825	Hygrine	0	39.42	0	Most abundant peak in 2 sprayed sample
13.392	n-Hexadecanoic acid	0	0.11	0	
15.607	cis-9-Hexadecenal	0	0.1	0	
15.042	Oleic Acid	0	0	0.21	

Table 4: GCMS – Fenugreek.

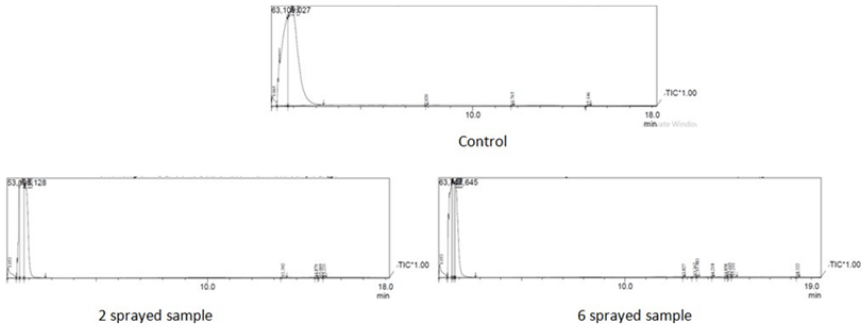

Figure 8: GCMS Fenugreek.

Cumin: The control sample contains many long chain fatty acid such oleic acid, palmitic acid and stearic acid. After 2 spraying, there was new peak of Chloroform & decrease in Palmitic and stearic acid with increase in Oleic acid. This is responsible for enhancement of taste, aroma and hotness. While 6 sprayed sample has shown unique peak of Cyclotetrasiloxane with increase in palmitic acid and oleic acid, this is responsible for loss in taste, aroma and hotness.

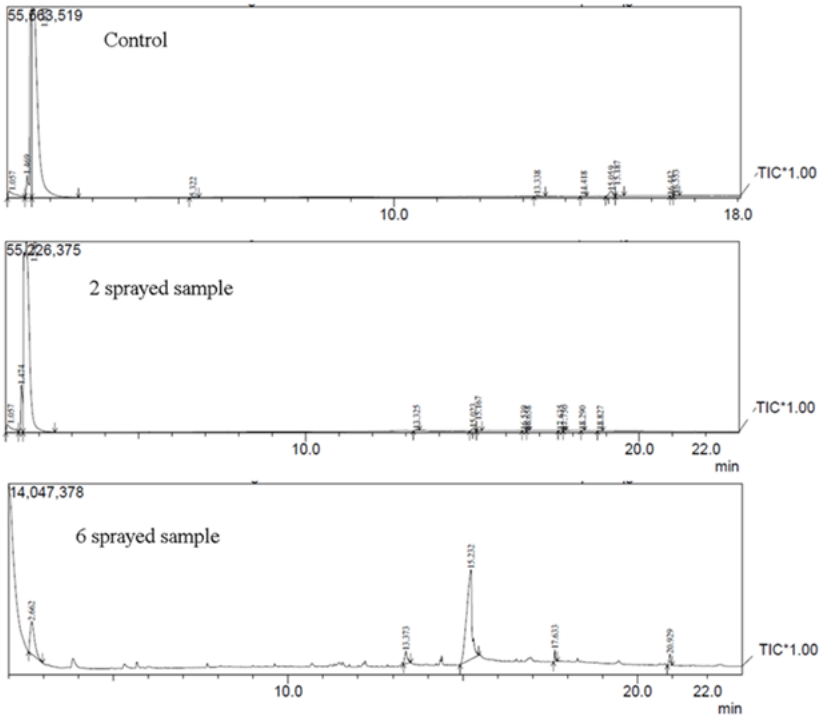

Figure 9: GCMS – Cumin.

R.T. (Min)	Name of Compound	% Area Present in each sample			Remarks
		Control	2 sprayed	6 sprayed	
1.057	9-Octadecenal, (Z)	2.85	3.42	0	
1.469	Acetone	24.53	7.23	0	
1.631	2,2'-Dipiperidine	70.73	0	0	Most abundant peak in control
1.546	Chloroform	0	88.26	0	Most abundant peak in 2 sprayed
2.26	Cyclotetrasiloxane	0	0	21.05	
13.338	n-Hexadecanoic acid (Palmitic acid)	0.28	0.15	4.54	
14.418	7-Octadecenoic acid, methyl ester	0.06	0	0	
15.059	6-Octadecenoic acid, (Z)- (Oleic acid)	1.07	0.53	0	
15.187	Octadecanoic acid (Stearic acid)	0.89	0.11	0	
15.233	6-Octadecenoic acid, (Z)- (Oleic acid)	0	0	69.97	Most abundant peak in 6 sprayed Antibacterial, anticancer, immune stimulant, anti- inflammatory (Mustapha et al., 2016; Helioswilton et al., 2013; European Patent Office, 2000)
17.633	Hexanoic acid, 2-ethyl-, 1,2-ethanediylbis(oxy-2,1-ethanediyl) ester	0	0	1.76	
20.92	Acethydrazide, N2-(2-ethyl-6-methyl)-	0	0	2.68	

Table 5: GCMS – Cumin.

Black Cumin:

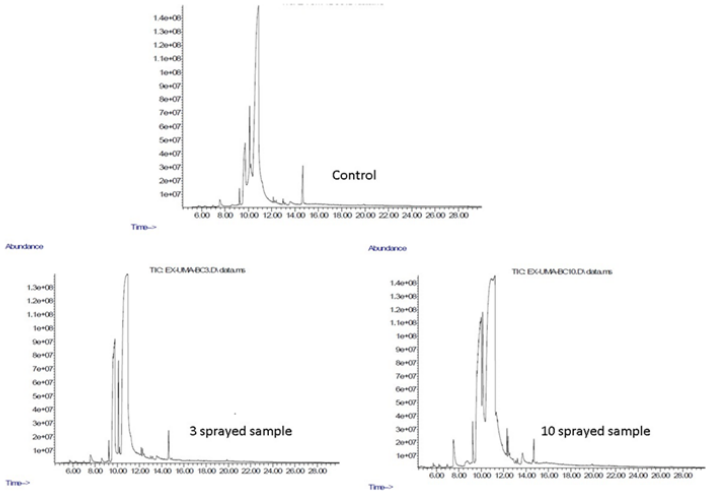

Figure 10: GCMS – Black cumin.

R.T. (Min)	Name of Compounds		
	Control	% Area	Remarks
7.476	Phenol, 4-methoxy-2,3,6-trimethyl-	0.62	The fatty acid and methyl esters of fatty acids were detected in control.
9.197	Hexadecanoic acid, methyl ester	0.45	
9.537	n-Hexadecanoic acid	9.41	The major fatty acid was Octadecadienoic acid (80 %)
10.02	Oxiraneoctanoic acid, 3-octyl-, cis-	6.54	
10.379	9,12-Octadecadienoic acid (Z, Z)-	80.36	
14.586	13-Docosenamide, (Z)-	2.59	
	3-sprayed		
7.457	Phenol, 4-methoxy-2,3,6-trimethyl	0.47	Common compounds as compared to control
9.206	Hexadecanoic acid, methyl ester	0.26	
9.5	n-Hexadecanoic acid	13.69	
10.048	8,11-Octadecadienoic acid, methyl ester	2.29	Unique Compound present in 3 and 10 sprayed sample
10.36	9,12-Octadecadienoic acid (Z, Z)-	82.71	Common compounds as compared to control
14.577	13-Docosenamide, (Z)-	0.548	
	10-sprayed		
7.504	Phenol, 4-methoxy-2,3,6-trimethyl	0.59	Common compounds as compared to control
9.178	Hexadecanoic acid, methyl ester	0.39	
9.547	n-Hexadecanoic acid	12.93	
10.067	8,11-Octadecadienoic acid, methyl ester	3.54	Unique Compound present in 3 and 10 sprayed samples
10.417	9,12-Octadecadienoic acid (Z, Z)-	81.61	Common compounds as compared to control
12.251	Hexadecanal, 2-methyl-	0.35	Unique Compounds present in 10 sprayed sample

12.383	Hexadecanoic acid, 3-[(trimethylsilyl)oxy] propyl ester	0.163	
14.653	13-Docosenamide, (Z)-	0.39	Common compounds as compared to control

Table 6: GCMS – Black cumin.

Coriander: The control sample contains many long chain fatty acid such oleic acid, palmitic acid and linoleic acid. After 2 spraying, there was new peak of Erucic acid, C-20 fatty acid & decrease in Linoleic acid. This is responsible for enhancement of taste, aroma and hotness. While 7 spraying has shown unique peak of Oleyl alcohol with increase in palmitic acid, this might be responsible for loss in taste, aroma and hotness. At RT (min) 15.442, 7 sprayed sample show oleyl alcohol peak of 58.66 which is absent in control and 2 sprayed samples. Biologically oleyl alcohol act as energy source and storage, nutrient and membrane stabilizer and in industry as surfactant and emulsifier. The lineoleic acid at RT (min) 15.502, 76.35% in control was disappeared completely by 2 and 6 sprayings whereas the same was naturally compensated by the reappeared lineoleic acid of 51.37% at RT (min) 15.433 by 2 spraying which is absent in control. The lineoleic acid is a source of energy and maintain fluidity of epidermal cell. At RT (min) 15.495 and 15.518 oleic acid is increased by 2 and 6 MIRGA sprayings respectively, but which is absent in control sample. This enhanced oleic acid posses beneficial health effects like anticancer, anti-inflammatory, wound healing, immune enhancing and macrophaging effects. On contrary, at RT (min) 15.558 control has oleic acid peak of 13.81% which was disappeared in 2 and 6 sprayed samples. Naturally, disappeared peak of 13.81% was compensated by 12.14% peak at RT (min) 15.555 by 6 sprayings but which is absent in control. At RT 15.596, 2 spraying has caused 12.66% peak of Erucic acid increase which is absent in control and 6 spraying. Though eruic acid long term intake (like; rape seed/mustard seed) acuse mycodial lipidosis but the effect is only transient and reversible hence safe.

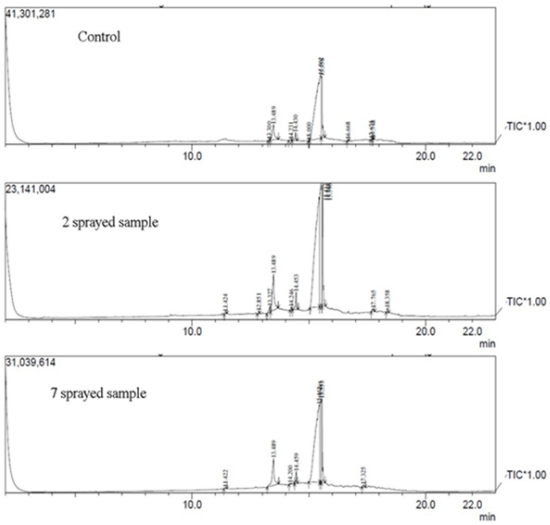

Figure 11: GCMS – Coriander.

R.T.(Min)	Name of Compound	% Area Present in each sample			
		Control	2 sprayed	7 sprayed	Remarks
13.489	n-Hexadecanoic acid (Palmitic acid)	6.98	7.15	8.79	
14.43	6-Octadecenoic acid, methyl ester	1.52	0	0	
14.453	6-Octadecenoic acid, methyl ester, (Z)	0	1.58	0	
14.459	6-Octadecenoic acid, methyl ester, (Z)	0	0	1.53	

15.502	9,12-Octadecadienoic acid (Z,Z)-(Linoleic Acid)	76.35	0	0	Most abundant peak in Control
15.433	cis,cis-Linoleic acid	0	51.37	0	Most abundant peak in 2 sprayed sample
15.442	Oleyl Alcohol	0	0	58.66	Most abundant and unique peak in 7 sprayed sample
15.495	6-Octadecenoic acid, (Z)-(Oleic acid)	0	0	17.83	
15.518	Oleic Acid	0	24.78	0	Most abundant peak in 2 sprayed sample Antibacterial, anticancer, immune stimulant, anti- inflammatory (Mustapha et al., 2016; Helioswilton et al., 2013)
15.555	6-Octadecenoic acid (Oleic acid)	0	0	12.14	
15.558	6-Octadecenoic acid, (Z)-	13.81	0	0	
15.596	Erucic acid	0	12.66	0	Unique peak in 2 sprayed sample

Table 7: GCMS – Coriander.

Cardamom:

RT (min)	Name of compounds	% area present in each sample			
		Control	2 sprayed	11 sprayed	Remarks
14.082	Eucalyptol	18.72	16.79	15.6	Common peak in all three samples
14.706	Eucalyptol	0	0	14.84	
14.735	Eucalyptol	12.6	11.22	0	
21.489	Cyclohexene, 1-methyl-4-(1-methylethylidene)	1.32	0.92	1.13	
26.21	3-Cyclohexen-1-ol, 4-methyl-1-(1- methylethyl)-, acetate	0	69.26	0	Most abundant peak in 2 sprayed sample
26.222	Cyclohexene, 1-methyl-4-(1- methylethylidene)	0	0	65.51	Most abundant peak in 11 sprayed smaple
26.2	3-Cyclohexene-1-methanol, α, α4-trimethyl	65.46	0	0	Most abundant peak in control
30.181	Naphthalene, 1,2,3,5,6,7,8,8a-octahydro-1,8a-dimethyl-7-(1- methylethenyl)-, [1S-(1α,7α,8aα)]	0.94	0.91	1.06	Common peak in all three samples
32.453	1H-Benzocycloheptene, 2,4a,5,6,7,8,9,9a-octahydro-3,5,5-trimethyl-9-methylene-, (4aS-cis)	0	0.87	0	
32.48	γ-HIMACHALENE	0.93	0	0.84	

Table 8: GCMS – Cardamom.

FTIR

Pepper: N-H stretching at 3415cm-1.Aliphatic C-H stretching at 2926cm-1and 2860cm-1.The peak at 1639cm-1 is due to C=O stretching. The peak at 1442cm-1 and 1556cm-1 is due to C-Cstr in aromatic ring. However there is no any significant difference in bond change parameters in between the samples. But the peak intensity due to N-Hstr and and C-H str is more in 2 sprayed than in 10 sprayed sample.

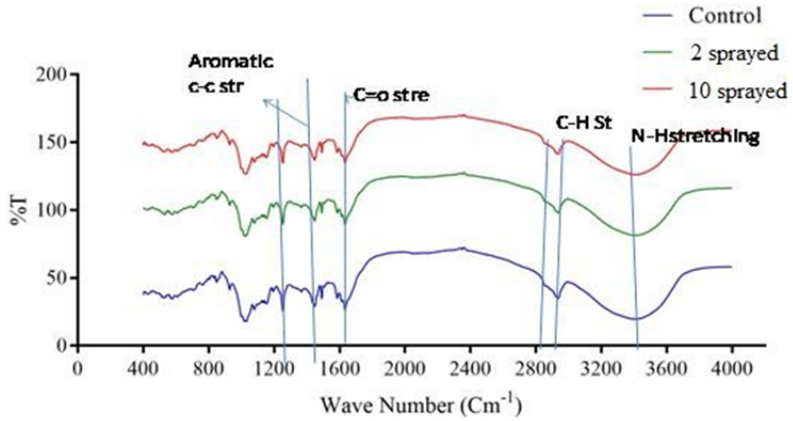

Figure 12: FTIR – Pepper.

Chili Pepper: Average Transmission Response in All Samples: The average transmission signal drops in the 6 sprayed sample. The signal then slightly increases again (by an average of 1.80%) in the 12 sprayed sample. Therefore, it could generally be understood that the spraying process increases the mid-infrared absorption in the sample. Control Sample: The absorption at ~2924 cm-1, seen amongst others in the functional group region, is associated with the stretching vibration of N-H [15] in the amine functional group.

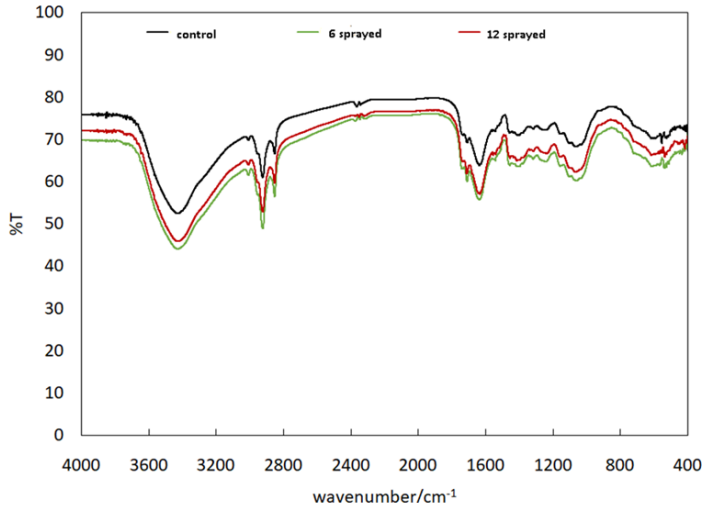

Figure 13: FTIR – Chilli Pepper.

- **6 Sprayed Sample:** There is no significant change in the fingerprint region compared to the control sample. In the functional group region however, in addition to a shift in the background signal, there is a signal jump of around 6% in the N-H stretching vibration at ~2924 cm-1.

- **12 Sprayed Sample:** There is no significant change in the fingerprint region compared to the control and 6 sprayed samples. In the functional group region however, in addition to a shift in the background signal, the signal shift in the N-H stretching vibration at ~2924 cm-1 drops again by around 2.5%. The observed changes in the N-H stretching vibration is interpreted as to the 6 sprayed sample being more favorable than the control sample, and the 12 sprayed sample being less favorable [15].

Ginger: Average Transmission Response in All Samples: The average transmission signal drops in the 2 sprayed sample by 4.42%. However, the signal slightly goes up again in the 8 sprayed sample showing an average drop of 3.27% compared to control. Following the same trend, the transmission signal in the 10 sprayed sample shows an average increase of 2.99% compared

to control. Therefore, assuming there are no significant irregularities in the measurements, following an initial increase the spraying process reduces the average mid-infrared absorption in the sample.

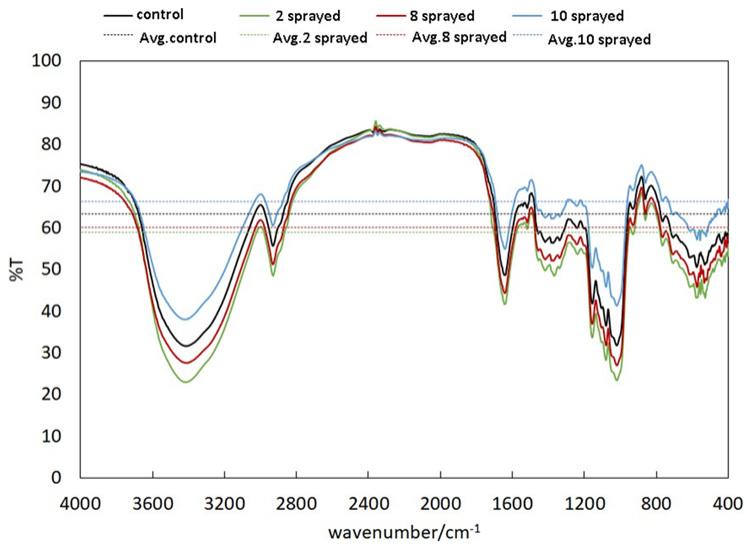

Figure 14: FTIR – Ginger.

- **Control Sample:** The broad signal in the range of 3200-3600 cm-1, seen amongst others in the functional group region, is associated with the stretching vibration of O-H [15] in the hydroxyl functional group of ginger.

- **2 Sprayed Sample:** There is no significant change in the fingerprint region compared to the control sample. In the functional group region however, in addition to a shift in the background signal, there is a signal jump of around 7.6% in the broad peak of the stretching vibration of O-H at the range 3200-3600 cm-1, hence increasing the O-H bond.

- **10 Sprayed Sample:** There is no significant change in the fingerprint region compared to the control and 2 sprayed samples. In the functional group region however, in addition to a shift in the background signal, the signal shift in the O-H stretching vibration of O-H at ~ 3200-3600 cm-1 drops again such that in the high treated sample the signal is around 6.4% lower than the control sample. The observed changes in the O-H stretching vibration may be interpreted as to the 2 sprayed samples being more favorable than the control sample, and the 10 sprayed sample being less favorable.

Curry Leaves:

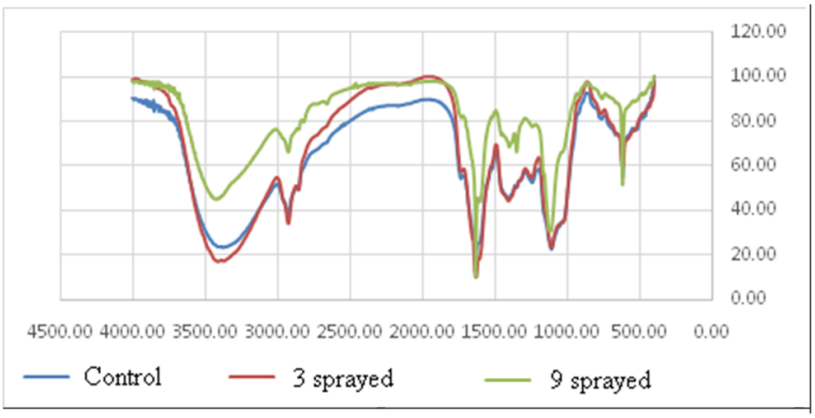

Figure 15: FTIR – Curry leaves.

- Peak 3408 cm-1 is responsible for the presence of the O-H here we can determine it as part of water peak and OH group from carbohydrates. Compared to control, in 3 sprayed sample square of this peak is bigger by 23%. In 9 sprayed sample square of this peak is smaller by 52%.
- Peak 2926 cm-1 is responsible for the presence of the C-H and is characteristic of carbon chain. Compared to control, in 3 sprayed sample square of this peak is bigger by 39%. In 9 sprayed sample square of this peak is smaller by 49%.
- Peak 2855 cm-1 is responsible for the presence of the C-H and is characteristic of carbon chain. Compared to control, in 3 sprayed sample square of this peak is bigger by 36%. In 9 sprayed sample square of this peak is smaller by 43%.
- Peak 1733 cm-1 is responsible for the presence of the C=0 here we can determine it as part of lipids. Compared to control, in 3 sprayed sample square of this peak is bigger by 5%. In 9 sprayed sample square of this peak is smaller by 68%.
- Peak 1633 cm-1 is responsible for the presence of the N-H here we can determine it as part of proteins. Compared to control, in 3 sprayed sample square of this peak is bigger by 27%. In 9 sprayed sample square of this peak is smaller by 41%.
- Peak 1112 cm-1 is responsible for the presence of the C-O group here we can determine it as part of carbonhydrates. Compared to control, in 3 sprayed sample square of this peak is bigger by 1%. In 9 sprayed sample square of this peak is smaller by 13%.
- Peak 1026 cm-1 is responsible for the presence of the C-O group here we can determine it as part of carbonhydrates. Compared to control, in 3 sprayed sample square of this peak is bigger by 5%. In 9 sprayed sample square of this peak is smaller by 64%.

Area of the peaks increased in 3 sprayed sample and reduced in 9 sprayed sample. MIRGA spraying reduced lipids and caused changes in carbohydrate structures.

Fenugreek:

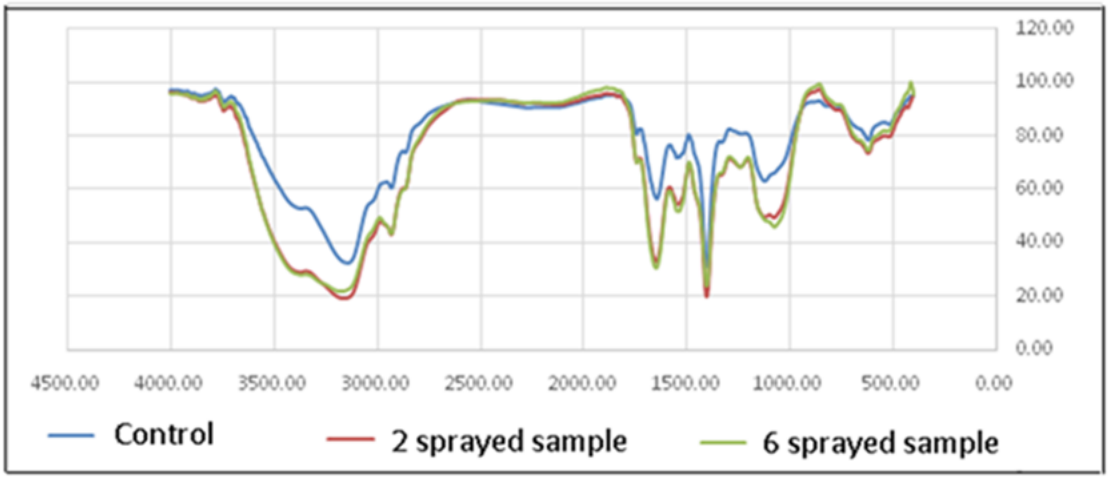

Figure 16: FTIR – Fenugreek.

- Peak 3374 cm-1 is responsible for the presence of the O-H here we can determine it as part of water peak. Compared to control, in 2 sprayed sample square of this peak is bigger by 107%. In 6 sprayed sample square of this peak is bigger by 117%.
- Peak 3143 cm-1 is responsible for the presence of the O-H, here we can determine it as characteric peak of carbohydrates. Compared to control, in 2 sprayed sample square of this peak is bigger by 58%. In 6 sprayed sample square of this peak is bigger by 54%.
- Peak 2930 cm-1 is responsible for the presence of the C-H and is characteristic of carbon chain. Compared to control, in 2 sprayed sample square of this peak is bigger by 111%. In 6 sprayed sample square of this peak is bigger by 128%.
- Peak 2860 cm-1 is responsible for the presence of the C-H and is characteristic of carbon chain. Compared to control, in 2 sprayed sample square of this peak is bigger by 36%. In 6 sprayed samplesquare of this peak is bigger by 19%.
- Peak 1746 cm-1 is responsible for the presence of the C=0 here we can determine it as part of lipids. Compared to control, in

2 sprayed sample square of this peak is bigger by 60%. In 6 sprayed sample square of this peak is bigger by 54%.

- Peak 1649 cm-1 is responsible for the presence of the N-H here we can determine it as part of proteins. Compared to control, in 2 sprayed sample square of this peak is bigger by 104%. In 6 sprayed sample square of this peak is bigger by 127%.
- Peak 1403 cm-1 is responsible for the presence of the CH2 group near C=O group here we can determine it as part of lipids. Compared to control, in 2 sprayed sample square of this peak is bigger by 35%. In 6 sprayed sample square of this peak is bigger by 24%.
- Peak 1122 cm-1 is responsible for the presence of the C-O group here we can determine it as part of carbonhydrates. Compared to control, in 2 sprayed sample square of this peak is bigger by 50%. In 6 sprayed sample square of this peak is bigger by 62,5%.
- Peak 1050 cm-1 is responsible for the presence of the C-O group here we can determine it as part of carbonhydrates. Compared to control, in 2 sprayed sample square of this peak is bigger by 83%. In 6 sprayed sample square of this peak is bigger by 116%.

In general, the peak area increases in 2 sprayed and 6 sprayed samples. Here with spraying rebuilding in the composition of carbohydrates occurred.

Cumin:

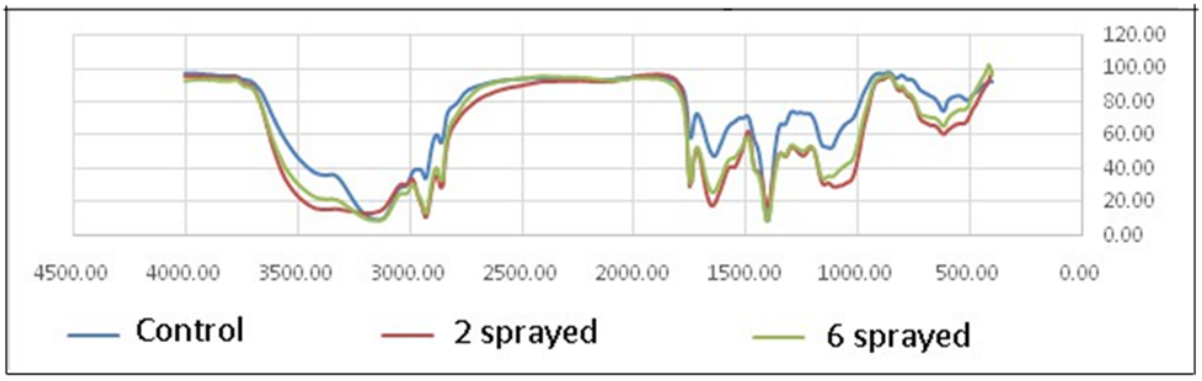

Figure 17: FTIR – Cumin.

- Peak 3374 cm-1 is responsible for the presence of the O-H here we can determine it as part of water peak. Compared to control, in sample square of this peak is bigger by 90%. In 6 sprayed sample square of this peak is bigger by 57%.
- Peak 3143 cm-1 is responsible for the presence of the O-H, here we can determine it as characteric peak of carbohydrates. Compared to control, in 2 sprayed sample square of this peak is smaller by 2%. In 6 sprayed sample square of this peak is smaller by 15%.
- Peak 2926 cm-1 is responsible for the presence of the C-H and is characteristic of carbon chain. Compared to control, in 2 sprayed sample square of this peak is bigger by 261%. In 6 sprayed sample square of this peak is bigger by 201%.
- Peak 2854 cm-1 is responsible for the presence of the C-H and is characteristic of carbon chain. Compared to control, in 2 sprayed sample square of this peak is bigger by 160%. In 6 sprayed sample square of this peak is bigger by 138%.
- Peak 1746 cm-1 is responsible for the presence of the C=0 here we can determine it as part of lipids. Compared to control, in 2 sprayed sample square of this peak is bigger by 121%. In 6 sprayed sample square of this peak is bigger by 113%.
- Peak 1645 cm-1 is responsible for the presence of the N-H here we can determine it as part of proteins. Compared to control, in 2 sprayed sample square of this peak is bigger by 150%. In 6 sprayed sample square of this peak is bigger by 75%.
- Peak 1403 cm-1 is responsible for the presence of the CH2 group near C=O group here we can determine it as part of lipids. Compared to control, in 2 sprayed sample square of this peak is smaller by 24%. In 6 sprayed sample square of this peak is bigger by 2%.
- Peak 1150 cm-1 is responsible for the presence of the C-O group here we can determine it as part of carbonhydrates. Compared to control, in 2 sprayed sample square of this peak is bigger by 61%. In 6 sprayed sample square of this peak is bigger by 47%.
- Peak 1050 cm-1 is responsible for the presence of the C-O group here we can determine it as part of carbonhydrates. In2 sprayed sample square of this peak is bigger by 206%. In 6 sprayed sample square of this peak is bigger by 113%.

In general, the peak area increases in 2 sprayed and 6 sprayed sample. In this case, 2 spraying caused a rebuilding in the composition of carbohydrates.

Black Cumin: The difference in the 3 spectra in 1658 cm−1 (corresponds to the C=O stretching) suggests changes in the C=O groups upon spraying. The decrease in the C=O can explain the reduced aroma of the 10 sprayed sample. There is peak at 1280 cm-1in the spectra of the 3 and 10 sprayed samples which is missing in the control sample. This peak corresponds to the CH3 bending, suggesting breakage of the molecule chain of the cumin upon spraying.

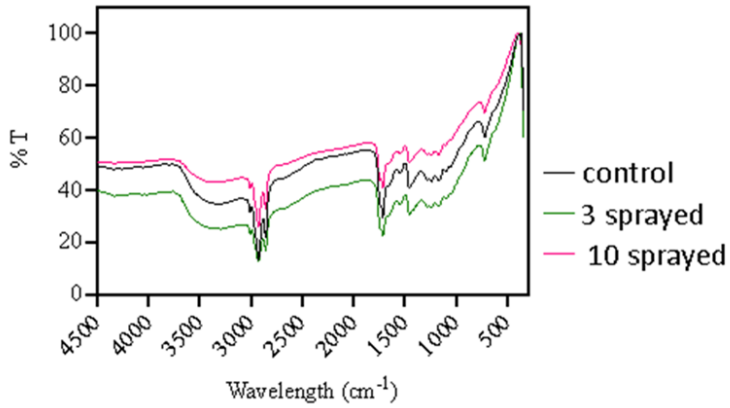

Figure 18: FTIR – Black cumin.

Coriander:

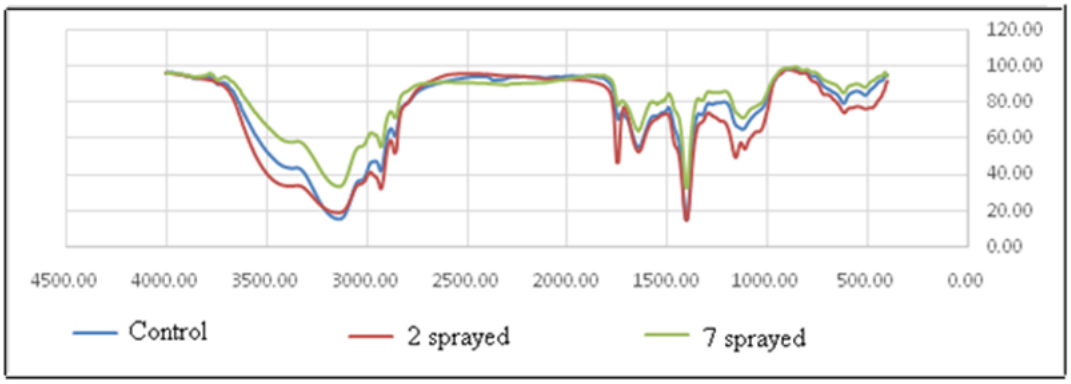

Figure 19: FTIR – Coriander.

- Peak 3384 cm-1 is responsible for the presence of the O-H here we can determine it as part of water peak. Compared to control, in 2 sprayed sample square of this peak is bigger by 42%. In 7 sprayed sample square of this peak is smaller by 39%.
- Peak 3134 cm-1 is responsible for the presence of the O-H, here we can determine it as characteric peak of carbohydrates. Compared to control, in 2 sprayed sample square of this peak is smaller by 3%. In 7 sprayed sample square of this peak is smaller by 41%.
- Peak 2931 cm-1 is responsible for the presence of the C-H and is characteristic of carbon chain. Compared to control, in 2 sprayed sample square of this peak is bigger by 50%. In 7 sprayed sample square of this peak is smaller by 20%.
- Peak 2858 cm-1 is responsible for the presence of the C-H and is characteristic of carbon chain. Compared to control, in 2 sprayed sample square of this peak is bigger by 38%. In 7 sprayed sample square of this peak is smaller by 38%.
- Peak 1746 cm-1 is responsible for the presence of the C=0 here we can determine it as part of lipids. Compared to control, in 2 sprayed sample square of this peak is bigger by 424%. In 7 sprayed sample square of this peak is smaller by 37 %.

- Peak 1641 cm-1 is responsible for the presence of the N-H here we can determine it as part of proteins. Compared to control, in 2 sprayed sample square of this peak is bigger by 3%. In 7 sprayed sample square of this peak is smaller by 17%.
- Peak 1403 cm-1 is responsible for the presence of the CH2 group near C=O group here we can determine it as part of lipids. Compared to control, in 2 sprayed sample square of this peak is bigger by 13%. In 7 sprayed sample square of this peak is smaller by 40%.
- Peak 1157 cm-1 is responsible for the presence of the C-O group here we can determine it as part of carbonhydrates. Compared to control, in 2 sprayed sample square of this peak is bigger by 313%. In 7 sprayed sample square of this peak is smaller by 34%.
- Peak 1100 cm-1 is responsible for the presence of the C-O group here we can determine it as part of carbonhydrates. Compared to control, in 2 sprayed sample square of this peak is bigger by 238%. In 7 sprayed sample square of this peak is smaller by 30%.
- Peak 1030 cm-1 is responsible for the presence of the C-O group here we can determine it as part of carbonhydrates. Compared to control, in 2 sprayed sample square of this peak is bigger by 165%. In 7 sprayed sample square of this peak is smaller by 7%.

The peak area increases in 2 sprayed sample and reduce in 7 sprayed. Here the most noticeable increase in the content of fats and carbohydrates with 2 sprays which, however, is not noticeable with 7 sprays.

Cardamom: The most remarkable change is the variation in the transmittance (absorption) that is directly related to the concentration. The control sample shows a broad band between 3700-3000 cm-1 which is attributable to O-H stretching of alcohols (probably, establishing hydrogen bonds). This band can also have the contribution of the stretching of N-H bonds from amines or amides. A more defined band appears between 2800- 3000 cm-1, which are typical of the C-H stretching of saturated moieties, like alkanes or cycloalkanes. Less intense peaks are observed between 1780-1500 cm-1 that could be originated by the stretching of C=O bonds. Below 1500 cm-1 the fingerprint region is located. This region is usually very crowded and it is difficult to identify peaks accurately. The 2 sprayed sample shows a spectrum with a significantly lower transmittance, pointing to a reduced concentration of the compounds giving rise to the observed bands. Bands and peaks observed in this sample are quite similar in shape and position compared to the control sample. A special reduction of the transmittance in the bands corresponding to the C-H stretching of saturated-1 moieties (2800-3000 cm) is observed in these samples. The 11 sprayed sample shows a spectrum with a significantly lower transmittance compared with the control sample, but higher than the transmittance of the 2 sprayed sample. These points to the fact that the reduction of the concentration of compounds giving rise to the peaks and bands is not so pronounced in 11 sprayed sample compared with 2 sprayed sample. Cardamom powder consists of a set of major components: carbohydrates (40 %), dietary fiber (30%), proteins (10 %), lipids (7 %). The composition is completed with many other minor components, such as vitamins, minerals, flavonoids, and the molecules responsible for aroma and taste of cardamom (mainly, terpenoids). Therefore, a FTIR spectrum of a cardamom sample is expected to display bands and peaks characteristic of the chemical groups presents in those molecules. These bands and peaks (only the most significant ones) are summarized in this table:

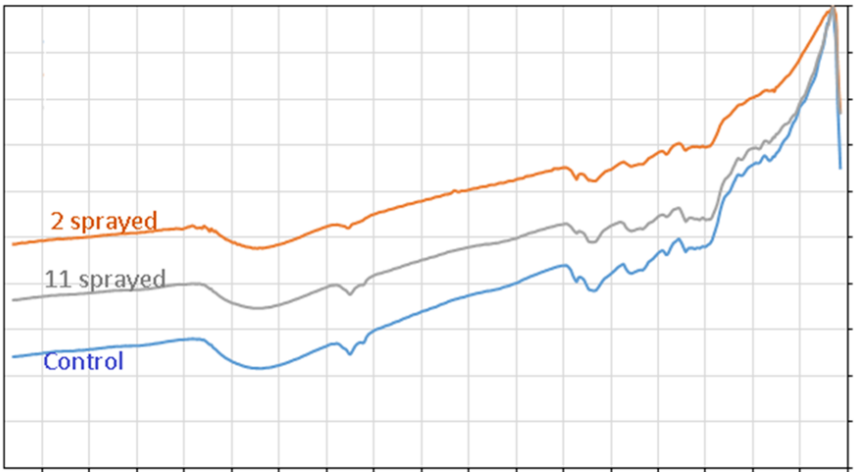

Figure 20: FTIR – Cardamom.

Compound	Assignment	Wavenumber (cm-1)
Carbohydrates	O-H stretching	3650-3200
	C-H stretching from saturated moieties (aliphatic and cyclic)	3090-2860
	CH2 bending	1475-1430
	CH3 bending (asymmetrical)	1470-1430
	CH3 bending (symmetrical)	1395-1365
	C-O stretching	1260-970
Proteins (backbone)	N-H stretching	3300-3070
	Amide I mode	1650
	Amide II mode	1550
	Amide III mode	1400-1200
Lipids	C-H stretching from saturated moieties	3090-2860
	C=H stretching (unsaturated fatty acids)	3095-3020
	C=O stretch from esters and acids	1750-1650
Terpenoids	O-H stretching	3650-3200
	C-H stretching from saturated moieties (aliphatic and cyclic)	3090-2860
	C=H stretching (cycloalkene)	3095-3020
	C=O stretching from ester	1790-1650
	C-O-C stretching (asymmetrical)	1310-1000

Table 9: FTIR spectrum analysis of a cardamom sample.

Moving the data from the table to the FTIR spectra of cardamom control sample:

Changes observed upon spraying of the cardamom sample affect to aroma, taste, and texture. Aroma and taste of cardamom come principally from a set of monoterpenoids which are widely identified in many scientific studies. These compounds are essentially α-terpinyl acetate, 1,8-cineol (eucalyptol), sabinene, α-terpinol, and limonene. Changes observed in the organoleptic properties of cardamom samples should be directly related to variations in the concentration of these compounds. In the case of 2 sprayed sample, that was irradiated two times with IR radiation, an increase of aroma and taste was observed, as well as a change in the sample texture, becoming softer. Observing the FTIR spectra, no variation in the number, type, and position of bands and peaks is spotted. This points to the fact that major components of the sample do not disappear or suffer chemical changes upon treatment. However, a drastic, general diminution of the transmittance occurs, indicating a decrease in the concentration of the major components of the sample, responsible for the main peaks and bands observed. A possible explanation to these observations is that treatment causes a reduction in the concentration of major components of the sample. If this reduction does not affect minor components, such as terpenoids, it results in the net augmentation of their concentration (since the total amount of components decreases, if the amount of terpenoids is maintained, their concentration will be higher). A higher concentration of these compounds that are responsible for aroma and taste of the sample, will lead to a strengthening of these organoleptic characteristics. In addition, as terpenoids are oil-like compounds, if their concentration increases, the sample probably will become softer. On the other hand, 11 sprayed sample was irradiated eleven times with IR radiation. The result was a reduced aroma and taste, and a texture identical to the control sample. Like in the case of 2 sprayed sample, observing the FTIR spectra, no variation in the number, type, and position of bands and peaks is spotted, pointing to the fact that major components of the sample do not disappear or suffer chemical changes upon treatment. In this case, a general decrease of transmittance is also observed respect to the control sample, but not so drastic compared to 2 sprayed sample. This means that, despite of being more irradiated, this sample do not lose as much amount of the main components as 2 sprayed sample. The causes behind this observation are difficult to elucidate. Perhaps, applying too many irradiation cycles causes changes in the sample structure, blocking in some point the loss of major components. However, the loss of aroma and taste could be explained considering that such a high number of irradiation cycles could lead to the elimination of the terpenoids, responsible for aroma and taste. These minor components are volatile and too much radiation will favor their release from the sample. In addition, the loss of these oil-

like compounds will impede the softening of the sample, and thus, it preserves the texture of the control sample.

PXRD

Pepper: Control: One broad peak is observed between 14.0° and 28.0°, comprised by several prominent and minor peaks. Five prominent peaks are observed first at 2θ = 11.5°, 15.1°, split peaks between 16.0° and 19.0°, 22.8°, and 25.9°. Other minor peaks observed are at 2θ = 17.3°, 18.3°, and 19.9°, and 29.9°. 2 sprayed sample: One broad peak is observed between 14.0° and 28.0°, comprised by several prominent and minor peaks. Four prominent peaks are observed first at 2θ = 15.1o, split peaks between 16.0° and 19.0°, 22.8°, and 26.2°. Other minor peaks observed are at 2θ = 17.3°, 18.2°, 21.6°, 28.3°, 29.8° and 30.4°

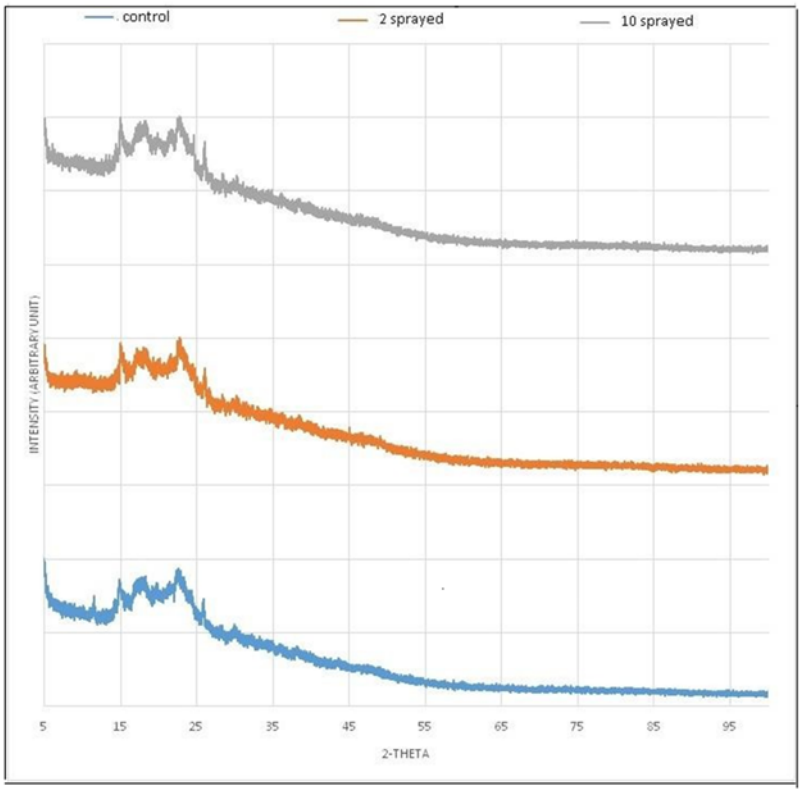

Figure 21: PXRD – Pepper.

- **10 sprayed sample:** One broad peak is observed between 13.5° and 28.5°, comprised by several prominent and minor peaks. Four prominent peaks are observed first at 2θ = 15.1o, split peaks between 16.0oand 19.0o (merging and centered at 18.4°), 22.8°, 24.6°, 26.1°. Other minor peaks observed are at 2θ = 17.4°, 19.9°, 21.8°, 24.6°, 28.5oand 30.4° Comparison of control, 2 sprayed and 10 sprayed samples: 10 sprayed sample has the most number of prominent peaks in its XRD among the three samples. Some of the peaks that are merged in both control and 2 sprayed samples' splits in 10 sprayed sample. Peak intensity around 26.00 increases with the increase in spraying. Peak of control around 11.0o is absent in 2 sprayed and 10 sprayed. New peak can be observed in 10 sprayed samples XRD at 24.0°. Both scenarios indicate formation of new phases in sprayed samples. The 2 sprayed and 10 sprayed samples show similar XRD while control sample show relatively broader diffraction.

- **Generalization:** Pepper sample is naturally crystalline. Presence of large background radiation at low 2-Theta values is due to several factors. Spread of beam across the whole sample where maximum number of possible crystallites are available to diffract the x-ray is one.

Chili Pepper: All three samples show broad peak centered at 21.5° slightly shifting to higher 20 values with the increase of sprayings.

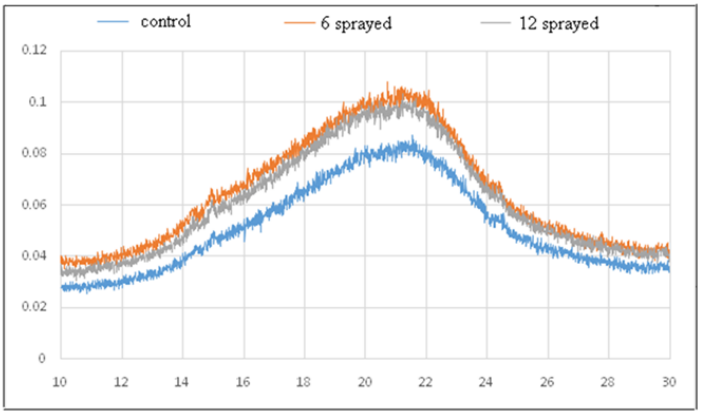

Figure 22: PXRD- Chilli Pepper.

Ginger: Patterns indicate that samples have amorphous and crystalline zones. Control, 2, 8 and 10 sprayed samples show broader peaks at 2θ: 15.12; 17.07; 18.01; 23.07; and 26.56. Small variations in relative intensity of signals at 2θ: 23.07 from 87% (Control), 87% (2 sprayed), 83% (8 sprayed) to 91% (10 sprayed) and 2θ: 26.56 from 58% (Control), 60% (2 sprayed), 76% (8 sprayed) to 65% (10 sprayed) are evidences of heterogeneity in the samples.

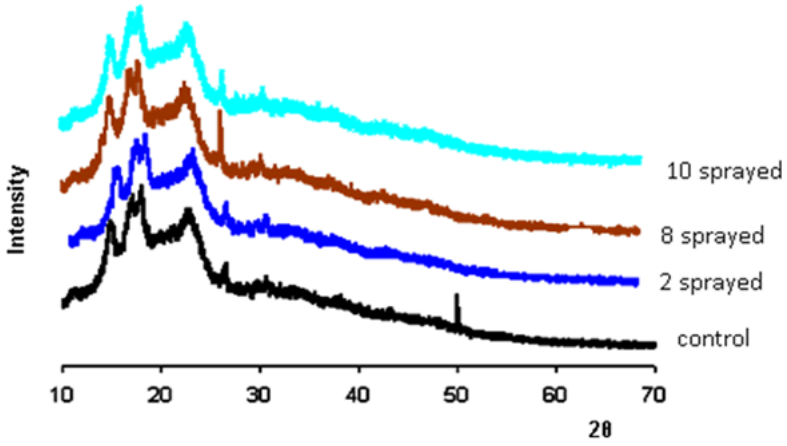

Figure 23: PXRD – Ginger.

	Relative intensity (I/Imax)%			
20	**Control**	**2 sprayed**	**8 sprayed**	**10 sprayed**
15.12	79	79	81	82
17.07	96	97	97	97
18.01	100	100	100	100
23.07	87	87	83	91
26.56	58	60	76	65

Table 10(a): PXRD analysis of ginger powder samples.

The areas under the peak in the range of 10o to 27o and the subsequent calculations for the purity of the product are as follows:

Percentage analysis of the change in Ginger powder				
	Control	**2 sprayed**	**8 sprayed**	**10 sprayed**
Peak at	10.0 -27.0	10.0 -27.0	10.0 -27.0	10.0 -27.0
Area	4489322	4340658	4365313	4037838
Change in area	0	-148663	-124008	-451483
Fraction change in area	0	-0,03311	-0,02762	-0,10057
Percentage change	0	-3,3	-2,8	-10,1

Table 10(b): PXRD analysis of ginger powder samples.

The result shows decreasing in the crystallinity of the powders by increasing the spraying. The 2 and 8 sprayed samples have decreased crystallinity by 3%. The 10 sprayed sample has a decreases crystallinity by 10%.

Curry Leaves:

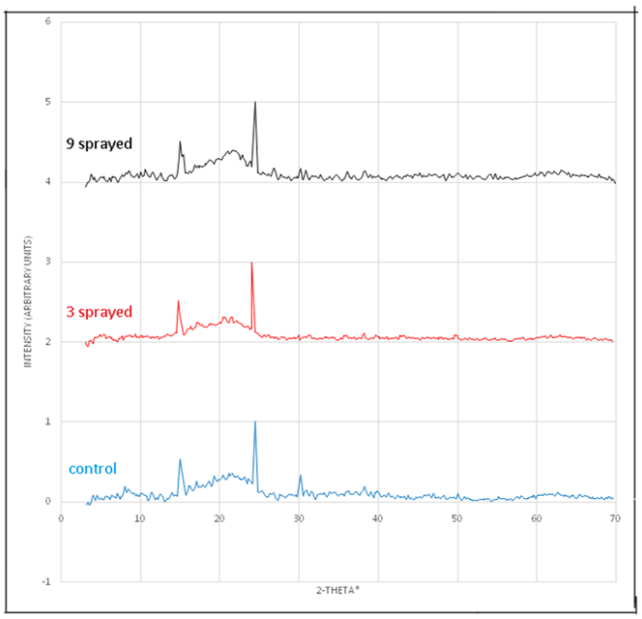

Figure 24: PXRD – Curry leaves.

- **Control:** One is a broad, diffused peak between 20 = 12° and 30°, maximum on 21.57° can be observed. Three prominent peaks are observed in the sample at14.95°, 24.44°, and 30.17°. Other minor peak is observed at 20= 38.28°.
- **3 sprayed:** Only two narrow, intense peaks can be seen at 20= 14.78° and 24.44°. A broad, diffused peak between 20 = 10° and 30°, centered on 20.69° is observed.
- **9 sprayed:** Two prominent peaks are observed in the sample. First are the split-peaks 14.97° and 15.38°, and second is the 24.43°. In between is a broad, diffused peak with its maximum at 21.99°. Other minor peaks are observed at 20 = 26.85°, 30.17°, and 30.82°.

- **Comparison of control, 3 and 9 sprayed samples' graphs:** Peaks in all three samples correspond to the data gathered in the literature. Control shows more prominent peaks than 3 sprayed and 9 sprayed. 3 sprayed shows two intense, narrow peaks. It also has the least intensity of broad peak at 20.69°. This indicates that 3 sprayed has more crystalline phase compared to control and 9 sprayed. Location of peak around14o is similar for control and 9 sprayed. Shifting to the left and splitting of this peak is observed in 3 sprayed. Peak at around 30° is observed in both control and 9 sprayed. Only 9 sprayed showed a peak at 26.85°.

Fenugreek:

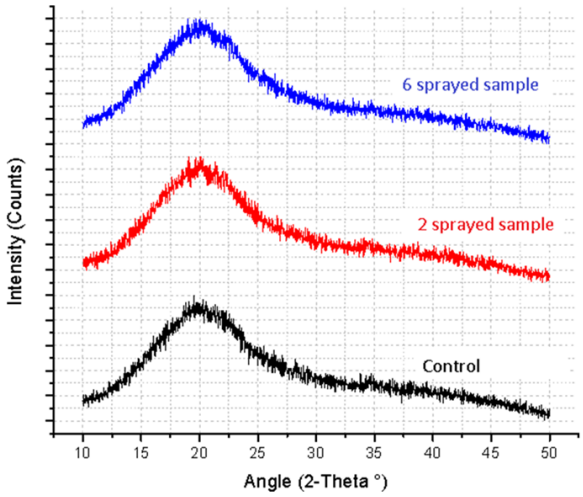

Figure 25: PXRD – Fenugreek.

- **Control:** Control spectrum exhibited a large bump between 10° and 32°. Broad diffraction peak implies that X-rays were scattered in many directions. Highest intensity was recorded at2θ= 19.5 (1196.67)
- **2 sprayed:** 2 sprayed spectrum exhibited a large bump between 10° and 32°. Broad diffraction peak implies that X-rays were scattered in many directions. Highest intensity was recorded at = 19.66 (1231.67)
- **6 sprayed:** 6 sprayed spectrum exhibited a large bump between 10° and 32°. Broad diffraction peak implies that X-rays were scattered in many directions. Highest intensity was recorded at 2θ= 20.04 (1290)
- **Comparison:** The XRD patterns of the control and the sprayed samples are relatively similar with each other. With this, it can be inferred that the spraying employed in the study retained the initial amorphous nature of the fenugreek sample. Generally, peak intensity variations can be accounted on crystallite sizes and non-random crystallite orientations. Raw fenugreek seed sample exhibits amorphous structure. Wherein fenugreek seed mucilage was studied. Amorphous materials do not have long-range atomic order therefore produce broad scattering peaks.

Cumin:

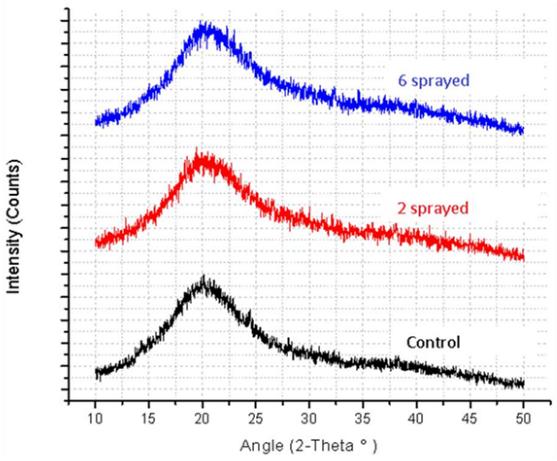

Figure 26: PXRD – Cumiin.

- **Control:** One broad peak is observed between 10.0o and 30.0o, with noticeable minor peak located at 2θ=24.46o. Broad diffraction peak implies that X-rays were scattered in many directions.

- **2 sprayed:** One broad peak is observed between 10.0o and 30.0o. Broad diffraction peak implies that X-rays were scattered in many directions.

- **6 sprayed:** One broad peak is observed between 10.0o and 30.0o. Broad diffraction peak implies that X-rays were scattered in many directions.

- **Comparison:** It can be observed that XRD signals of the samples exhibit broad diffraction patterns with large amount of noise. This behavior indicates amorphous nature of the samples. Broad peak observed on the range of 2θ seen in each spectrum indicates presence of cellulosic contents. Peak of control around 2θ=24.46o is absent in 2 sprayed and 6 sprayed. This scenario indicates that treated samples exhibit formation of new phases.

Intensity of the XRD spectrum differs for each sample. Generally, peak intensity variations can be accounted on crystallite sizes and non-random crystallite orientations.

Black Cumin:

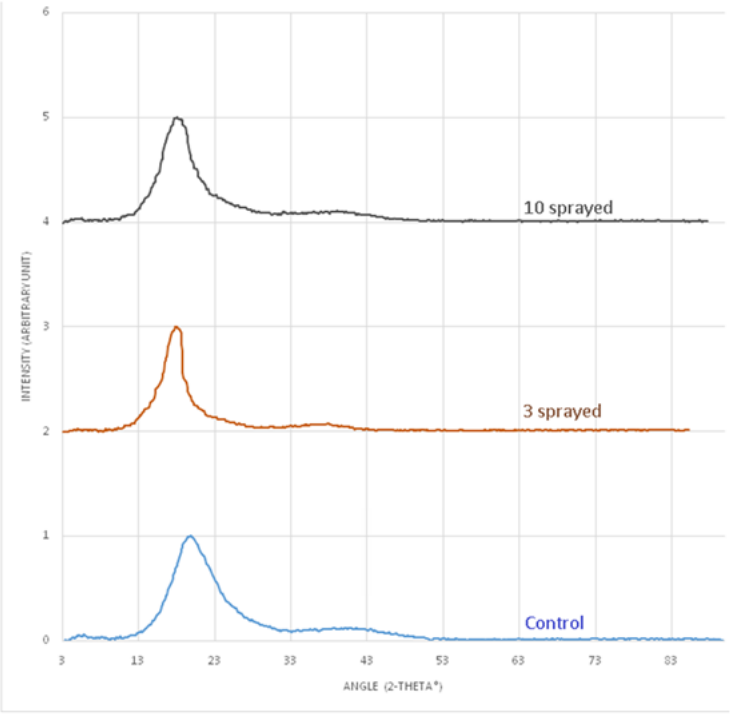

Figure 27: FTIR – Black cumin.

- **Control:** One broad peak is observed between 10.00o and 50.00o, comprised by some prominent and weak broad peaks. One strong, broad peak is observed between 20 values 10.00o and 33.00o. A weak, broad signal can also be observed between 20 values 33.00o and 50.00o Maximum intensity peak can be observed at 20 = 19.83

- **3 sprayed sample:** One broad peak is observed between 13.00o and 50.00o, comprised by some prominent and weak broad peaks. One strong,bold peak is observed between 20 values 10.00o and 33.00o. A weak, broad signal can also be observed between 20 values 35.00o and 48.00o Maximum intensity peak can be observed at 20 = 19.53

- **10 sprayed sample:** One broad peak is observed between 10.00o and 48.00o, comprised by some prominent and weak

broad peaks. One strong, broad peak is observed between 20 values 13.00o and 33.00o. A weak, broad signal can also be observed between 20 values 33.00o and 51.00o Maximum intensity peak can be observed at 20 = 19.64

- **Comparison of the samples:** 3 sprayings produced a narrower intense peak compared to the control. 10 sprayings produced a broader intense peak compared to the control. These scenarios may indicate the significant effect of the number of MIRGA sprayings on the resulting crystallite size of the samples.

- **Generalization:** The XRD patterns of the three samples exhibited broad peaks between 2θ values 10° and 50°. From molecular aspect, these broad peaks are linked to the cellulosic content of the samples. Furthermore, the weak peaks can be attributed to the amorphous nature of black cumin.

Coriander:

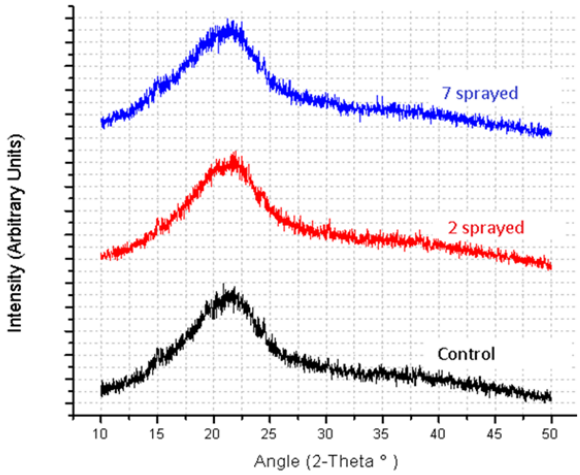

Figure 28: PXRD – Coriander.

- **Control:** One broad peak is observed between 10.0o and 30.0o with noticeable minor peaks located at2θ=15 o and 24.42 oBroad diffraction peak implies that X-rays were scattered in many directions.

- **2 sprayed:** One broad peak is observed between 10.0o and 30.0o with noticeable minor peaks Located at2θ=15 o and 24.42 o. Broad diffraction peak implies that X-rays were scattered in many directions.

- **7 sprayed:** One broad peak is observed between 10.0o and 30.0o with noticeable minor peaks located at2θ=15.02 o and 24.48o. Broad diffraction peak implies that X-rays were scattered in many directions.

- **Comparison:** The XRD patterns of the control and the sprayed samples are relatively similar with each other. With this, it can be inferred that the sprayings employed in the study retained the initial amorphous nature of the coriander samples. Generally, peak intensity variations can be accounted on crystallite sizes and non-random crystallite orientations.

- **Generalization:** Coriander samples exhibit amorphous structure. This is mainly due to the presence of cellulose, specifically lignin as its major component. Amorphous materials do not have long-range atomic order therefore produce broad scattering peaks. Based from the generated spectra, initial structures of the control coriander sample were maintained even after subjected to sprayings (2 sprayed and 7 sprayed).

Cardamom:

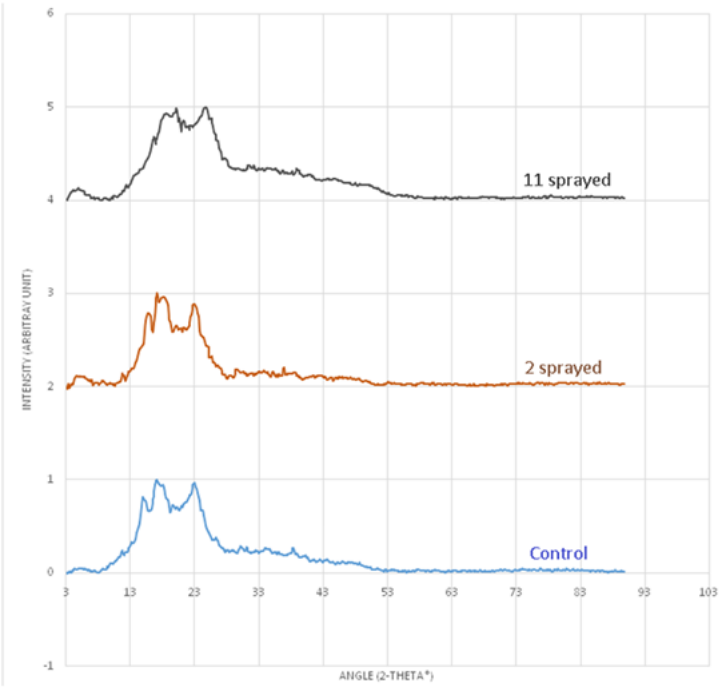

Figure 29: PXRD – Cardamom.

- **Control:** One broad peak is observed between 8.00o and 50.00o, comprised by several prominent and minor peaks.Three prominent peaks are observed first at 20 = 15.05o, 17.31o and 22.80o A minor peak can be observed at 20= 5.50oOther minor peaks overriding the broad signal are observed at 20=31.07o, 34.55oand 38.24.

- **2 Sprayed Sample:** One broad peak is observed between 10.00o and 50.00o, comprised by several prominent and minor peaks. Three prominent peaks are observed first at 20 = 15.03o, 16.88o and 22.54o A minor peak can be observed at 20= 5.51o. Other minor peaks overriding the broad peak are observed at 20=30.14o and37.98.

- **11 Sprayed Sample:** One broad peak is observed between 10.00o and 55.00o, comprised by several prominent and minor peaks. Two prominent peaks are observed first at 20 = 18.49o and 23.32o. A minor peak can be observed at 20= 5.05oOther minor peaks overriding the broad peak are observed at 20=31.29o and 38.89o.

- **Comparison:** The three samples exhibited considerably similar XRD patterns except that some peaks present on the control are not observed on the two experimental samples. Peak around 2q = 15.00o is absent at 11 sprayed sample. Peak around 2q = 34.00o is absent at 2 and 11 sprayed samples. These absences indicate differences in crystal structure of the samples.

- **Generalization:** Cardamom seeds consist of perisperms and endosperms which are filled with starch grains. Based from related literatures, the XRD patterns of the three cardamom samples in this study agree with the signature diffraction signals and peaks of organic materials with starch components. The XRD patterns also indicate mixture of crystalline and amorphous phases in the sample.

NMR

Pepper: One of the main compositions of pepper is piperine, and the chemical shift of the axially substituted cyclohexane at 3.528 ppm remains the same in (control) and (2 sprayed) and (10 sprayed), we can use this peak as a reference to normalize the integral values in all the three data. With respect to the control sample, the monosubstituted alkane–COOCH3 (0.918 ppm), the monosubstituted alkane–phenyls (1.602 and 2.343 ppm), the conjugated dienes (5.976 ppm), the saturated alicyclic

hydrocarbons (6.420 ppm) decrease in the 2 sprayed sample. But in the 10 sprayed sample these integrals increase again. The peak integral chart shows the same behavior for the axially substituted cyclohexane at 3.528 ppm. Hence interpreted as to the 2 sprayed sample being more favorable than the control sample and the 10 sprayed sample being less favorable.

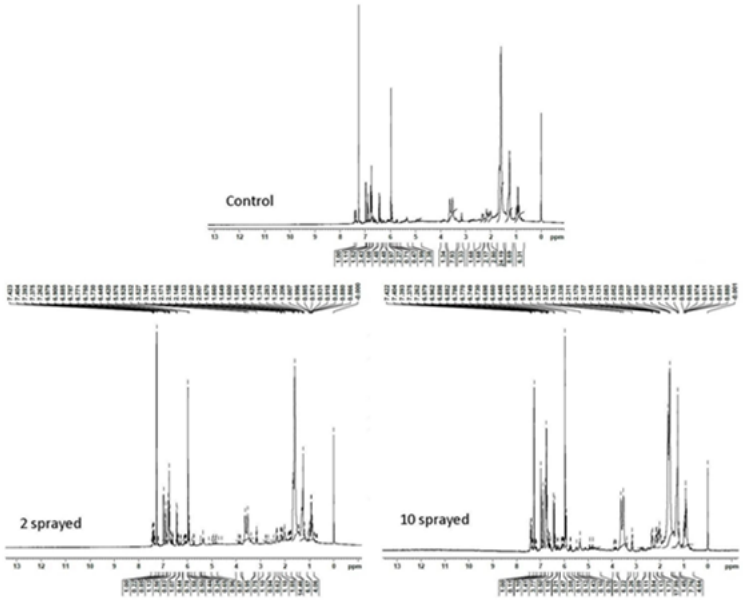

Figure 30: NMR – Pepper.

Chemical Shift Description			Control			2 sprayed sample			10 sprayed sample		
			Chemical Shift (ppm)	Peak Integral	Normalized Peak Integral	Chemical Shift (ppm)	Peak Integral	Normalized Peak Integral	Chemical Shift (ppm)	Peak Integral	Normalized Peak Integral
Monosubstituted Alkanes	–COOCH3	Alkyl group -2-Propyl	0.918	6.31	0.8	0.918	4.06	0.68	0.917	4.64	0.75
Monosubstituted Alkanes	–phenyl	Alkyl group -2-Propyl	1.255	8.69	1.1	1.254	6.57	1.1	1.254	7.76	1.25
Monosubstituted Alkanes	–phenyl	Alkyl group - n-Butyl	1.602	24.19	3.05	1.6	14.46	2.43	1.597	17.99	2.89
Axially Sub stituted Cyclohexanes	– NHCOCH3	Alicyclic s	2.008	2.8	0.35	2.007	1.85	0.31	2.007	1.73	0.28
Monosubstituted Alkanes	–COCH3	Alkyl group - Methyl	2.171	2.17	0.27	2.171	1.1	0.18	2.17	1.13	0.18
Monosubstituted Alkanes	–phenyl	Alkyl group -Methyl	2.343	1.68	0.21	2.342	0.62	0.1	2.338	0.84	0.14
unknown in control sample					0	2.457	0.94	0.16	2.457	0.11	0.02

Carbonyl Derivatives	H4C2(CO2) 2NH	Carboxy lic Acid Imides	2.77	1.68	0.21	2.77	1.1	0.18	2.77	0.09	0.01
Monosubstituted Et hylenes	–OCH3	Alkenes	3.164	1.33	0.17	3.164	0.75	0.13	3.163	0.26	0.04
Axially Sub stituted Cyclohexanes	–OH,–tert-butyl	Alicycli cs	3.528	7.93	1	3.527	5.95	1	3.527	6.22	1
Monosubstituted Alkanes	–NC	Alkyl group - 2-Propyl	3.914	1.34	0.17	3.913	0.87	0.15	3.91	0.17	0.03
Substituted Ethylenes		Alkenes	4.941	2.38	0.3	4.941	0.96	0.16	4.939	0.7	0.11
MonosubstitutedEt hylenes	–NC	Alkenes	5.348	1.99	0.25	5.348	0.65	0.11	5.347	0.43	0.07
unknown in control sample					0	5.467	0.24	0.04	5.485	0.12	0.02
Substituted Ethylenes		Alkenes	5.758	0.47	0.06	5.758	0.44	0.07	5.76	0.11	0.02
Conjugated Dienes		Alkenes	5.929	0.71	0.09	5.928	0.5	0.08	5.928	3.05	0.49
Conjugated Dienes		Alkenes	5.976	2.27	0.29	5.976	1.58	0.27	5.975	3.05	0.49
Substituted Ethylenes	–COOCH3	Alkenes	6.1	0.97	0.12	6.099	0.78	0.13	6.098	0.47	0.08
Ketones		Carbony l Compounds	6.294	0.48	0.06	6.293	0.44	0.07	6.292	0.21	0.03
Saturated Alicyclic Hydrocarbons		Alicycli cs	6.42	1.48	0.19	6.42	1.07	0.18	6.419	1.18	0.19
Amides of Aliphatic Carboxylic Acids		Amides and Lactams	6.618	1.08	0.14	6.617	0.83	0.14	6.616	0.5	0.08
Saturated Alicyclic Hydrocarbons		Alicycli cs	6.75	3.43	0.43	6.75	2.56	0.43	6.749	3.77	0.61
MonosubstitutedEt hylenes	–2-naphthyl	Alkenes	6.885	1.52	0.19	6.885	1.13	0.19	6.882	1.41	0.23
unknown peak			6.98	1.11	0.14	6.979	0.85	0.14	6.979	1.1	0.18
unknown in control sample					0	7.183	0.22	0.04	7.182	0.11	0.02
Carboxylic Acid Esters		Esters and Lactones	7.404	1	0.13	7.404	1	0.17	7.404	1	0.16

Table 11: 1H-NMR analysis of pepper powder samples.

Chili Pepper: Chili powder is mainly made up of capsaicin, and there is no significant change in the –NH compound at 0.880 ppm in control, 6 sprayed and 12 sprayed samples, we can use this peak as a reference to normalize the integral values in all the three data sets. With respect to the control sample, the amines and ammonium salts at 1.301 and the monosubstituted alkane at 1.621 ppm and 2.347 ppm increase in the 6 sprayed sample. But in the 12 sprayed sample these integrals drop in value again. The peak shows a consistent drop in the –NH compound reference at 0.880 as the spraying increases. The rest of the spectral peaks show insignificant changes in the three samples. Hence interpreted as to the 6 sprayed sample being more favorable than the control

sample and the 12 sprayed sample being less favourable.

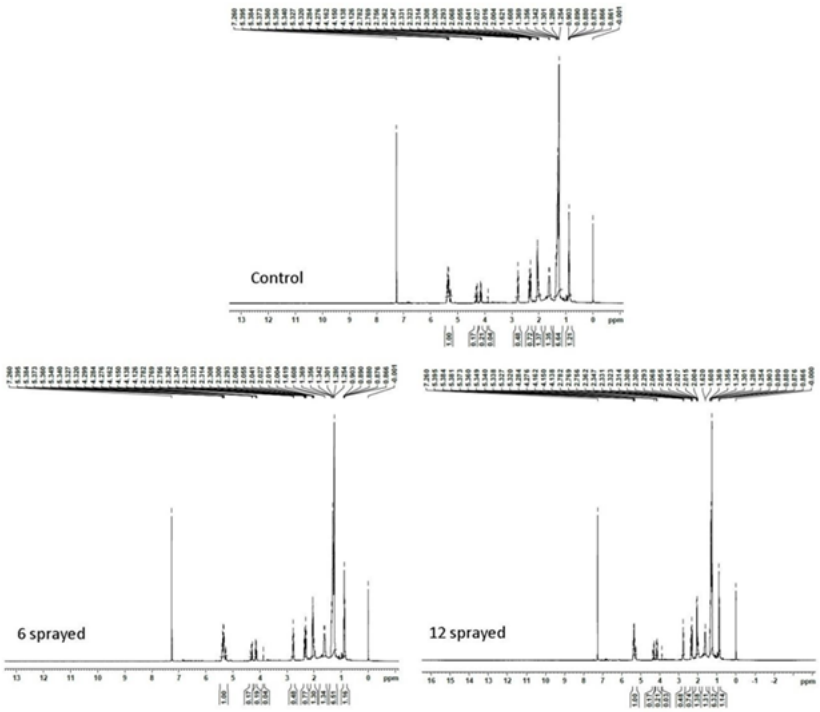

Figure 32: NMR – Chili Pepper.

Chemical Shift Description			Control			6 sprayed			12 sprayed		
			Chemical Shift (ppm)	Peak Integral	Normalized Peak Integral	Chemical Shift (ppm)	Peak Integral	Normalized Peak Integral	Chemical Shift (ppm)	Peak Integral	Normalized Peak Integral
Amines and Ammonium Salts	-NH		0.88	1.21	1	0.88	1.16	1	0.88	1.14	1
Amines and Ammonium Salts	0		1.301	6.64	5.49	1.301	6.51	5.61	1.301	6.32	5.54
Monosubstituted Alkanes	–COOH	Alkyl group - n-Butyl	1.621	1.35	1.12	1.619	1.34	1.16	1.62	1.31	1.15
Amides of Aliphatic Carboxylic Acids		Dimethyl Sulfoxide (DMSO)	2.041	1.37	1.13	2.041	1.3	1.12	2.041	1.38	1.21
Monosubstitut ed Alkanes	–phenyl	Alkyl group – Methyl	2.347	0.72	0.6	2.347	0.77	0.66	2.347	0.74	0.65
Carbonyl Derivatives	H4C2(CO 2)2NH	Carboxylic Acid Imides	2.769	0.48	0.4	2.769	0.48	0.41	2.769	0.48	0.42
Monosubstituted Alkanes	–NC	Alkyl group - 2- Propyl	3.878	0.04	0.03	3.878	0.04	0.03	3.878	0.03	0.03

Formamides		Amides and Lactams	4.15	0.21	0.17	4.15	0.19	0.16	4.15	0.21	0.18
Carbohydrates		Dimethyl Sulfoxide (DMSO)	4.3	0.17	0.14	4.299	0.17	0.15	4.299	0.17	0.15
Monosubstitut edEthylenes	–NC	Homoallylic Coupling	5.36	1	0.83	5.36	1	0.86	5.36	1	0.88

Table 12: 1H-NMR of chili powder.

Ginger: The main composition of ginger is zingiberene, and there is no change in the chemical shift and the integral of monosubstituted alkanes–OCO–phenylat 3.872 ppm in (control) and (2 sprayed) and (8 sprayed) and (10 sprayed), we can use this peak as a reference to normalize the integral values in all the four data. As can be seen in the normalized peak integral chart, with respect to the control sample, the fatty acid CH3 (0.879 ppm), the monosubstituted alkane –phenyl (1.254 ppm), the axially substituted cyclohexane (1.584 ppm), the saturated alicyclic hydrocarbons (2.051 and 2.186 ppm), the substituted alkane (2.841 ppm), and the substituted ethylene (6.816 ppm)decrease in the 2 sprayed sample. But in the 8 sprayed and 10 sprayed samples & these integrals increase again, apart from the substituted ethylene (6.816 ppm) which continues dropping consistently. Hence interpreted as to the 2 sprayed sample being more favorable than the control sample, and the 8 sprayed and 10 sprayed samples being less favorable.

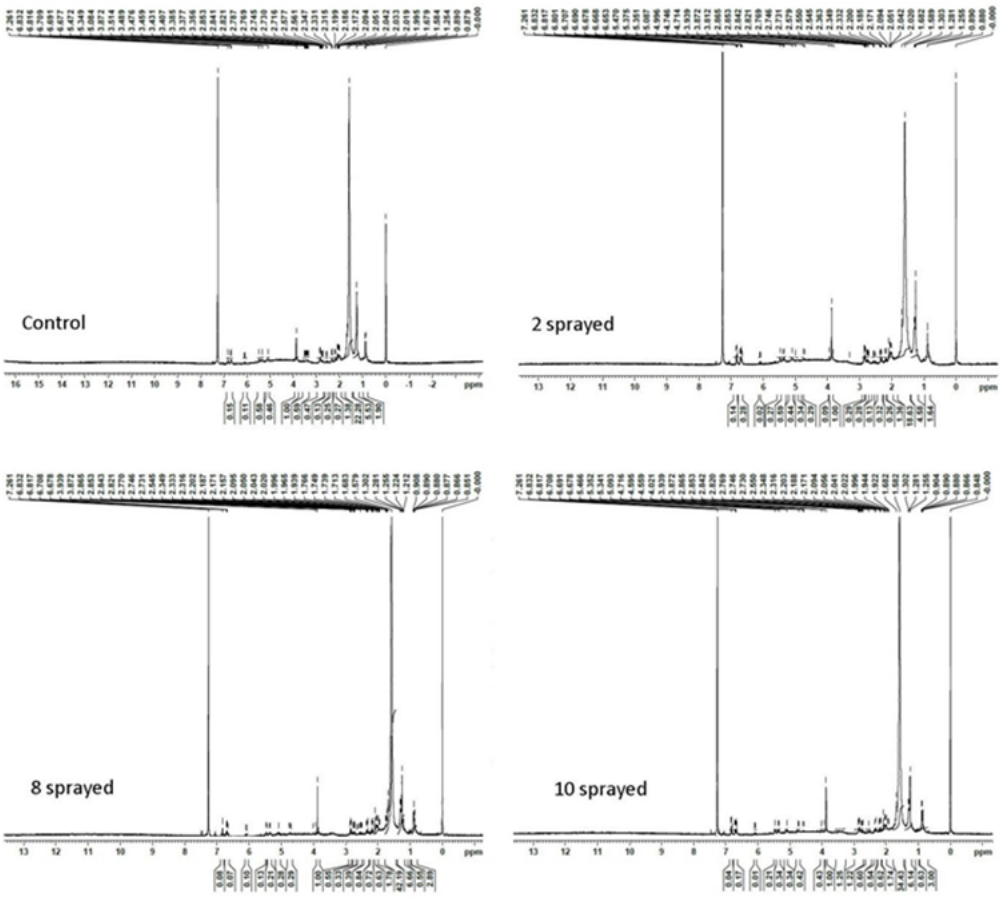

Figure 33: NMR – Ginger.

Chemical Shift Description			Control			2 sprayed Sample			8 sprayed Sample			10 sprayed Sample		
			Chemical Shift (ppm)	Peak Integral	Normalized Peak Integral	Chemical Shift (ppm)	Peak Integral	Normalized Peak Integral	Chemical Shift (ppm)	Peak Integral	Normalized Peak Integral	Chemical Shift (ppm)	Peak Integral	Normalized Peak Integral
Fatty acid	CH3	Alkyl group - Ethyl	0.879	1.9	1.9	0.88	1.64	1.64	0.88	2.89	2.89	0.88	3	3
Monosubstituted Alkanes	–phenyl	Alkyl group - 2- Propyl	1.254	5.53	5.53	1.255	4.58	4.58	1.255	6.66	6.66	1.255	6.14	6.14
Axially Substituted Cyclohexanes	–C	Alicycl ics	1.584	22.2	22.28	1.589	18.6	18.63	1.579	42.1	42.19	1.582	34.4	34.43
Saturated Alicyclic Hydrocarbons		Alicycl ics	2.051	1.38	1.38	2.051	1.36	1.36	2.05	1.78	1.78	2.056	1.74	1.74
Saturated Alicyclic Hydrocarbons		Alicycl ics	2.186	0.27	0.27	2.185	0.26	0.26	2.187	0.63	0.63	2.188	0.62	0.62
Monosubstituted Alkanes	–phenyl	Alkyl group -Methyl	2.331	0.25	0.25	2.332	0.32	0.32	2.333	0.84	0.84	2.348	0.54	0.54
Ketones		Carbonyl Compounds	2.577	0.13	0.13	2.579	0.13	0.13	2.58	0.39	0.39	2.55	0.6	0.6
Substituted Alkanes	–O– CO–	Alkanes	2.841	0.47	0.47	2.769	0.28	0.28	2.77	0.33	0.33	2.842	1.22	1.22
Substituted Alkanes	–O– CO–	Alkanes	2.841	0.47	0.47	2.842	0.29	0.29	2.843	0.55	0.55	2.842	1.22	1.22
Monosubstituted Alkanes	–O– phenyl	Alkyl group -Ethyl	3.431	0.59	0.59			0			0	3.39	1.25	1.25
Monosubstituted Alkanes	– OCO – phenyl	Alkyl group - Methyl	3.872	1	1	3.872	1	1	3.872	1	1	3.872	1	1
unknown in control sample					0	3.939	0.09	0.09			0	3.939	0.43	0.43
unknown in control sample					0	4.746	0.29	0.29	4.744	0.29	0.29	4.745	0.42	0.42
unknown in control sample					0	4.996	0.34	0.34			0			0
unknown peak			5.084	0.46	0.46	5.087	0.44	0.44	5.088	0.28	0.28	5.093	0.34	0.34
unknown in control sample					0		0.59	0.59	5.36	0.21	0.21	5.352	0.34	0.34
unknown peak			5.472	0.58	0.58	5.47	0.27	0.27	5.466	0.13	0.13	5.466	0.21	0.21
Substituted Ethylenes	– COOCH3	Alkenes	6.104	0.11	0.11	6.104	0.02	0.02	6.105	0.1	0.1	6.105	0.01	0.01
Substituted Ethylenes	–OCOCH3	Alkenes	6.816	0.15	0.15	6.678	0.28	0.28	6.678	0.07	0.07	6.678	0.17	0.17
Substituted Ethylenes	–OCOCH3	Alkenes	6.816	0.15	0.15	6.817	0.14	0.14	6.817	0.08	0.08	6.817	0.04	0.04

Table 13: H-NMR analysis of ginger powder samples.

Curry Leaves:

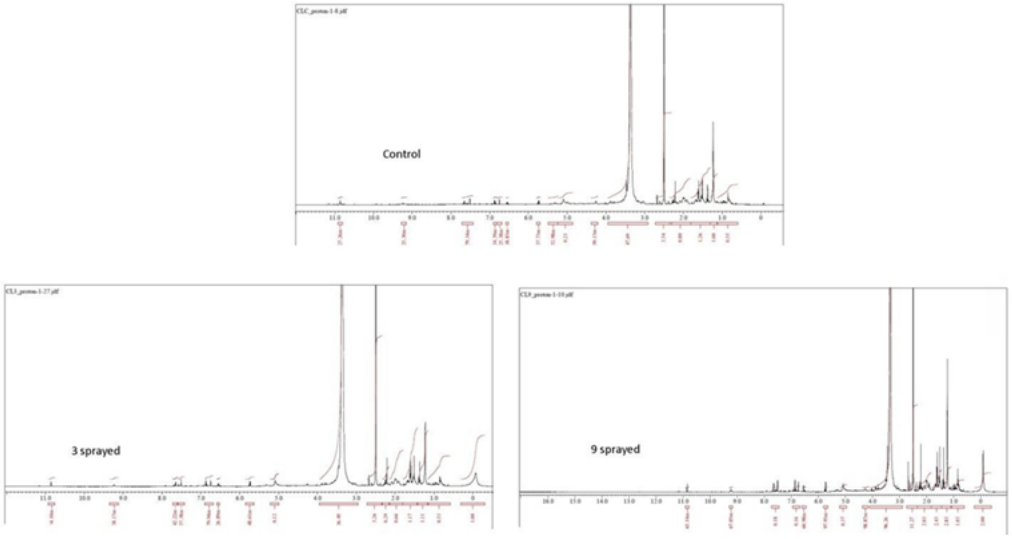

Figure 34: 1H-NMR of curry leaves powder.

- **Control**

Curry leaves contains a very high number of chemical compounds. They have a big amount of fiber that forms a non-soluble fraction, and a wide variety of substances, including terpenes, carbohydrates, amino acids, glycosides, flavonoids, plant sterols, vitamins, etc. In the scientific literature, the extraction with organic solvents applied on curry leaves generates a mixture of compounds that is especially rich in terpenes. Some of the most abundant terpenes identified in curry leaf extracts are β-caryophillene, 3- carene, α- and β-pinene, α-selinene, β-elemene, cymene, β-phellandrene, linalool, linalyl acetate, myrcene, and geranyl acetate.

It is expected to found signals corresponding to the previously mentioned compounds in the 1H NMR spectrum of the sample. However, it is a very complex task to find out the origin of the signals present in the spectrum since the components of this sample are very diverse. For example, terpenes form a huge family of chemical species that possess very different structures, sizes, and functional groups. For this reason, depending on the type of terpene considered, its NMR signals can be distributed in very different ways, because of the functional groups present in the molecule.

Analyzing the 1H NMR spectrum, we can observe two signals with very high intensity. One corresponds to the solvent (DMSO, δ = 2.50 ppm), and the other one comes from the residual water (δ = 3.36 ppm). In this case, a third intense signal is observed around 1.23 ppm and, together with the signals around 0.80 ppm, they may be originated by a contamination with grease (as mentioned in the previous sample). This contamination is quite common in samples that have undergo a purification process.

The signals located between 0 and 3.00 ppm (A) include those coming from methyl, methylene, and methine groups; allylic, arylic, and olefinic hydrogens; and alcohols. All these groups can be find in molecules such as terpenes or plant sterols. For example, β-caryophillene has their allylic protons around 1.60 ppm; 3-carene has arylic protons around 1.00 and 1.60 ppm; β-pinene has their allylic protons around 1.65 ppm; linalool has their allylic protons around 1.60-1.70 ppm and its hydroxylic proton around 2.00 ppm; etc.

The region between 3.00 and 5.00 ppm (B) could show signals corresponding to hydrogens from carbohydrates (between 3-4 ppm for ring hydrogens, around 5 ppm for anomeric protons). Between 4.5 and 5.5 ppm (C), olefinic protons are found, this is hydrogens attached to double bonds, which are present in every terpene molecule.

Flavonoids and terpenes usually contain conjugated double bonds or aromatic moieties. The hydrogens attached to these regions are located between 5.5 and 8.0 ppm (D). Around 9 ppm (E), protons directly attached to carbonyl groups are found (aldehydes), and protons from carboxylic groups can be located between 10 and 12 ppm (F).

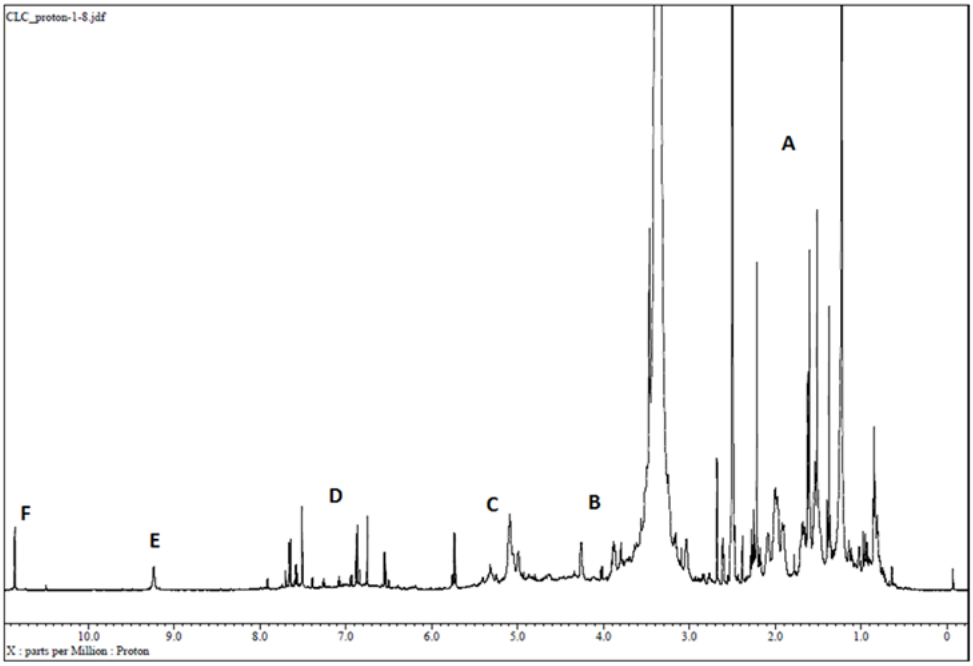

Figure 35: Analysis of 1H-NMR of curry leaves powder.

- **3 Sprayed Sample:** The organoleptic changes observed are: Taste increased and aroma increased. From the point of view of the NMR spectrum, the changes observed respect to the control sample are summarized in the next table:

Signals Control δ (ppm)	Signals 3 sprayed δ (ppm)	Signal integral Control	Signal integral 3 sprayed	Integral change
-0.07	-0.07	-	1	-*
0.60-1.15	0.60-1.15	0.55	0.53	-0.02
1.15-1.30	1.15-1.30	1	1.11	0.11
1.30-1.80	1.30-1.80	1.26	1.17	-0.09
1.80-2.30	1.80-2.30	0.8	0.95	0.15
2.40-2.75	2.40-2.75	3.54	3.26	-0.28
2.90-3.95	2.90-3.95	47.69	36.49	-11.2
4.20-4.40	4.20-4.40	0.005013	-	-*
4.85-5.25	4.85-5.25	0.21	0.12	-0.09
5.25-5.50	5.25-5.50	0.005298	-	-*
5.70-5.80	5.70-5.80	0.003773	0.004861	0.001
6.50-6.60	6.50-6.60	0.001883	0.002689	0.001
6.70-6.90	6.70-6.90	0.005977	0.007999	0.002
7.40-7.75	7.40-7.75	0.007934	0.00996	0.002
9.15-9.30	9.15-9.30	0.00253	0.003817	0.001
10.8-10.9	10.8-10.9	0.002726	0.00341	0.001

Table 14: NMR spectrum analysis of 3 sprayed curry leaves powder.
* This signal was not integrated in all spectra.

At first sight, comparing the two spectra (control and 3 sprayed sample), apparently, no signals disappear and no new signals are observed. This means that no drastic chemical transformations leading to the generation of new species have occurred upon 3 spraying. However, many signals show remarkable variations in their integrals pointing to the fact than some compounds have suffered alterations in their concentrations (some increased, others decreased).

First, a residual signal at -0.07 ppm in the spectrum of the control sample becomes significantly intense in this 3 sprayed sample. A negative chemical shift could arise from hydrogen's affected by the vicinity of aromatic moieties in molecules with certain molecular complexity, such as the ones mentioned in the previous section.

There is a general increase in the integral of every signal, pointing to a higher concentration of the corresponding chemical compounds. There is a remarkable reduction of the intensity in the integral of the signals located in the region 2.90-3.95 ppm but, as explained before, since this region contains the signal from residual water, any variation in the content of water in the sample will cause a visible change in this integral.

Since terpenes are very abundant in this kind of extracts, and these molecules are known for having strong odors, it is obvious that they are the main responsible for the organoleptic characteristics of the curry leaves powder. Any transformation that modifies the concentration or the properties of terpenes will cause a variation of aroma and taste in the sample. In the case of this 3 sprayed sample, the general augmentation of the integral values points to a higher concentration of terpenes, explaining the observed intensification of the taste and aroma.

- **9 sprayed sample:** The organoleptic changes observed are: Tasteless and aroma reduced. From the point of view of the NMR spectrum, the changes observed respect to the control sample are summarized in the next table:

Signals Control δ (ppm)	Signals 9 sprayed δ (ppm)	Signal integral Control	Signal integral 9 sprayed	Integral change
-0.07	-0.07	-	2	-*
0.60-1.15	0.60-1.15	0.55	1.03	0.48
1.15-1.30	1.15-1.30	1	2.83	1.83
1.30-1.80	1.30-1.80	1.26	2.43	1.17
1.80-2.30	1.80-2.30	0.8	2.03	1.23
2.40-2.75	2.40-2.75	3.54	11.27	7.73
2.90-3.95	2.90-3.95	47.69	96.26	48.57
4.20-4.40	4.20-4.40	0.005013	0.009887	0.005
4.85-5.25	4.85-5.25	0.21	0.37	0.58
5.25-5.50	5.25-5.50	0.005298	-	-*
5.70-5.80	5.70-5.80	0.003773	0.003773	0
6.50-6.60	6.50-6.60	0.001883	0.006098	0.004
6.70-6.90	6.70-6.90	0.005977	0.16	0.15
7.40-7.75	7.40-7.75	0.007934	0.18	0.19
9.15-9.30	9.15-9.30	0.00253	0.006705	0.004
10.8-10.9	10.8-10.9	0.002726	0.006514	0.004

Table 15: NMR spectrum analysis of 9 sprayed curry leaves powder.
* This signal was not integrated in all spectra.

At first sight, comparing the two spectra (control and 9 sprayed sample), apparently, no signals disappear and no new signals are observed. This means that no drastic chemical transformations leading to the generation of new species have occurred upon 9 spraying. However, many signals show remarkable variations in their integrals pointing to the fact than some compounds have suffered alterations in their concentrations.

First, a residual signal at -0.07 ppm in the spectrum of the control sample becomes significantly intense in this 9 sprayed sample, as observed in the 3 sprayed sample.

There is a general increase in the integral of every signal, which is even higher than the one observed in the 3 sprayed sample. This could make difficult the interpretation of the intensification of aroma and taste observed in the 3 sprayed sample, as a correlation with the augmentation of the concentration of terpenes. Regarding this explanation, in this case, with higher values of the integrals, a more intense aroma and taste will be expected, but this is not happening. In fact, there is a loss of aroma and taste.

It is possible that the 9 sprayings applied to sample is degrading some of the compounds responsible for the aroma and taste, but that their signals are overlapped with those from other compounds. If this compounds increase their concentration upon 9 sprayings, the decrease in the signals of the compound responsible for aroma and taste could be masked.

Conclusion

Control sample shows a profile compatible with a complex mixture of organic molecules, such as terpeneoids. This kind of compounds are the main contributor to the sensorial characteristics of curry leaves.

In this context, both 3 and 9 sprayed samples show variations in the NMR signals which are the cause of the modification of aroma and taste. Due to the overlap and the crowded spectra, it is difficult to accurately identify which signals are directly related to the changes observed in taste and aroma. In any case, the sprayings are acting on terpenoid molecules, reducing, increasing or modifying them in a way that strongly affects the organoleptic features of the curry leaves powder.

Fenugreek

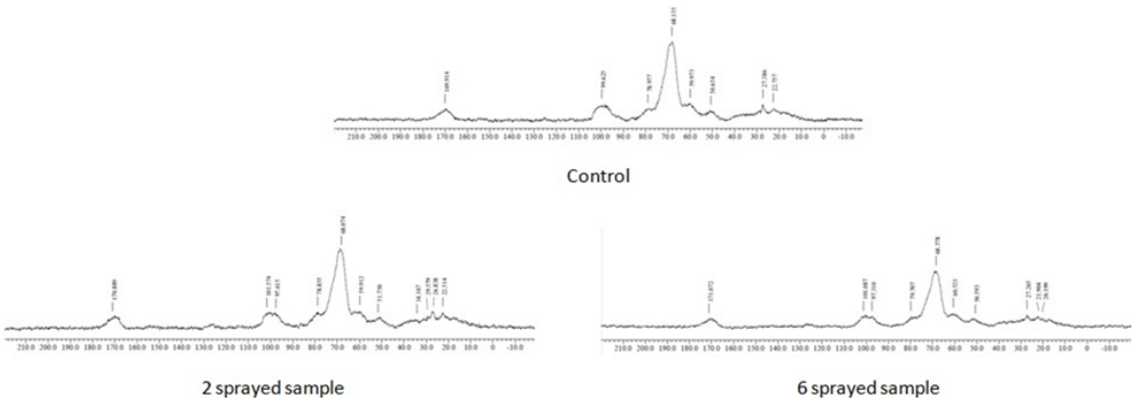

Figure 36: 13C Solid state NMR – Fenugreek.

Control	2 sprayed	6 sprayed	Typical Assignment
169.9 (broad)	170.9 (broad)	171	C=O (acids, esters)
99.6 (possible spinning sideband)	101.6 (possible spinning sideband)	101.1 (possible spinning sideband)	-
-	97.6	97.3	
79 (possible spinning sideband)	79 (possible spinningsideband)	79 (possible spinning sideband)	-
68.1 (intense resonance, slight peak split, doublet)	68.1 (intense resonance, slight peak split, triplet)	68.3 (intense resonance, slight peak split doublet)	RCH2O-

60 (possible spinning sideband)	60 (possible sideband)	60 (possible sideband)	-
50.6 (possible spinning sideband)	51.7(possible spinning sideband)	50.6 (possible spinning sideband)	-
-	34.1	-	CH3CO-, RCH2NH2
	29.6	-	CH3CO-, R3CH
	26.8	-	CH3CO-, R3CH
27.4	-	27.3	CH3CO-, R3CH
		21.9	R2CH2., CH3CO-
22.8	22.5		R2CH2., CH3CO-
		20.2	R2CH2., CH3CO-

Table 16: 13C solid state NMR analysis of Fenugreek.

Fenugreek seeds contain 4% moisture, 6.50% fiber, 3.20% ash, 28.55% protein, 4% fat, and 62.48% carbohydrates. Fenugreek leaves contain phenolic compounds, phenolcarbonic acids, chlorophylls, trigonoline and alkaloids. The phenolic compounds are typically glycosides. Researchers have detected beta-dl-arabinopyranose, sucrose, raffinose, glycerol, oxyacetic, succinic, 2,3-dioxypropanoic, 2,3,4- threehydroxybutyric acids and fatty palmitic and alpha- linolenic acids in fenugreek leaves. The following compounds were detected in fenugreek essential oil: hexadecene, eicozanol, ethyl palmitate, ethylinoleate, beta-hydroxy-butyric,beta- aminoizobutyric, hydroxybutanedicarbonic, 1,2,3-propanethreecarbonic acids; ethyl esters of linoleic, levulinic, palmitic, ethylpalmitic, citric acids, which are likely to form a spicy-aromatic flavor.

- **Control:** shows resonances associated with these classes of compounds and functional groups: acids, esters, RCH2O-, CH3CO-, and R3CH, and R2CH2. These functional groups and classes of compounds are consistent with the reported chemical compositions of fenugreek seeds and leaves below.
- **2 sprayed sample:** Compared to the control sample spectra, the absence of apparent resonance at 27.4 ppm and additional apparent resonances at 34.1 and 29.6 ppm might be indicator of compounds that reduce the bitterness of the 2 sprayed sample.
- **6 sprayed sample:** Compared to the control sample spectra, the additional apparent resonances at 21.9 ppm and 20.2 ppm may indicated changes in the 6 sprayed sample that lead to the lost of the bitter taste.

Cumin

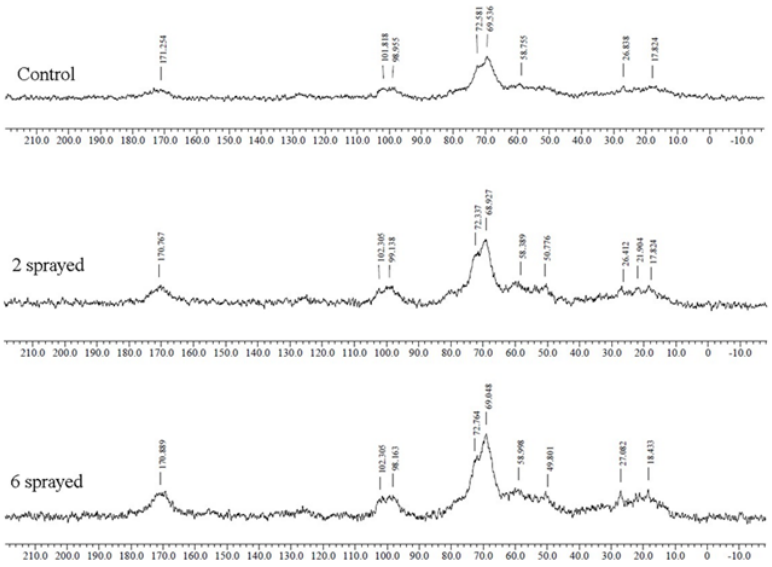

Figure F37: 13C Solid state NMR – Cumin.

Control	2 sprayed	6 sprayed	Typical Assignment
171.2 (broad, low int)	170.8 (broad, low/med int)	170.9 (med int)	C=O (acids, esters)
101.8 overlap with 98.9 (broad, low in)	102.3 overlap with 99.1 (broad, low/med int)	102.3 overlap with 98.1 (broad, low/med int)	C=C (alkenes)
69 with shoulder at 72 (highest intensity)	69 w/ shoulder at 72 (high int)	69 w/ shoulder at 72 (high int)	RCH2O-
58.7 (very low int)	58.4 (low int)	59 (low int)	RCH2O-
-	50.8 (low int)	49.8 (low int)	RCH2NH2, RCH2O-
26.8 (very low int)	26.4 (low int)	27.0 (med/low int)	R3CH
-	-	18.4 (med int)	R2CH2
-	21.9 (low int)	-	R2CH2, CH3CO-
17.8 (very low int)	17.8 (low int)		R2CH2

Table 17: 13C solid state NMR analysis of Cumin.

The key compounds in jeera powder are cuminaldehyde, cymene, and terpenoids. Other compounds in jeera powder that provide its aroma include substituted pyrazines, 2-ethoxy-3- isopropylpyrazine, 2-methoxy-3-sec-butylpyrazine, and 2-methoxy-3-methylpyrazine. Jeera powder may also contain γ-terpinene, safranal, p-cymene, and β-pinene. The C-13 CPMAS spectrum suggest key differences in the composition of each sample. Cuminaldehyde gives jeera powder its spiciness. And the following compounds may be associated with the flavors in jeera powder: beta-pinene (citrus), beta-pinene (cumin), cuminal (cumin), phenyethyl alcohol (floral), 1-hexanal (green), isopropolyquinoline (herbal), menthol (cooling), spearmint (cooling), isopropyl quinoline (earthy), and terpineol (sweet).

- **Control:** suggests the presence of these classes of compounds and functional groups: C=O, alkenes, RCH2O-, R3CH, R2CH2, and CH3CO-. The possible presence of a RCH2NH2 is suggested. However, this is not consistent with the reported chemical composition of jeera powder summarized in the paragraph directly below. The other classes of compounds and functional groups above are consistent with the chemical description of jeera powder.
- **2 sprayed sample:** The additional resonance in this sample 21.9 ppm relative to the control and apparent increase in intensity of the resonances suggests a more complex number of flavor compounds in the J2 sample compared to the control.
- **6 sprayed sample:** As 6 sprayed sample is tasteless, it may be lacking cuminaldehyde which perhaps is related to the absence of the peak at 17.8 ppm compared to the control.

Black Cumin:

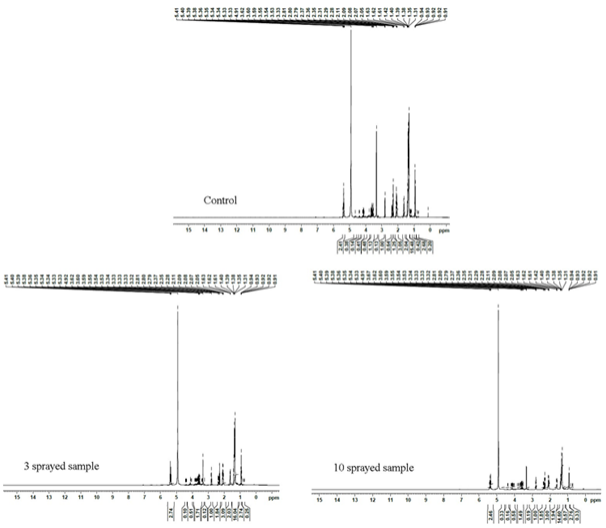

Figure 38: 1H-NMR – black cumin.

&5.4 (m, 1H),4.6 (s, 1H), 4.4 (q, 1H), 4.4 (m, 1H), 3.6 (m, 1H), 2.4 (m, 3H), 2.3 (t, 3H), 2.1 (m, 1H), 1.6(t, 1H), 1.3(d, 2H), 0.9 (t, 3H)

The 1H NMR spectra of the "black cumin" reveals the presence of a three proton singlet for CH3 group in aromatic rings, peak of three-proton intensity at δ0.9 for CH3. It also showsCH2 group at δ1.2. The CH3 group resonances are attributed to the different CH3 groups. The sharp peak at δ4.9 is due to the solvent (MeOD) and the sharp peak at about δ3.3 is due to the water.

In order to distinguish between the 3 samples, the peak integral of each samples were normalized. The number of CH3(and CH3 aromatic) groups are the same in all samples. However, there is slight decrease in the CH2 groups and slight increase in the CH groups in 10 sprayed sample suggesting some changes in the seed structure upon spraying.

Chemical Shift (ppm)	Control		3 sprayed sample		10 sprayed sample		Peak assigned
	Peak Integral	Normalized Peak Integral	Peak Integral	Normalized Peak Integral	Peak Integral	Normalized Peak Integral	
0.9-1.1	2.68	3	2.74	3	2.76	3	CH3
1.1-1.5	15.9	16	16.04	16	15.17	15	CH2
1.5- 1.7	2.04	2	2.03	2	1.94	2	CH
1.9-2.2	3.05	3	3.09	3	3	3	CH3 ar
2.3-2.4	1.89	2	1.84	2	1.85	2	CH3 ar
2.7-2.8	1		1		1		
4.0-5.5	3.2	3	3.4	3	3.9	4	CH

Table 17: NMR spectrum analysis of Black cumin.

Coriander

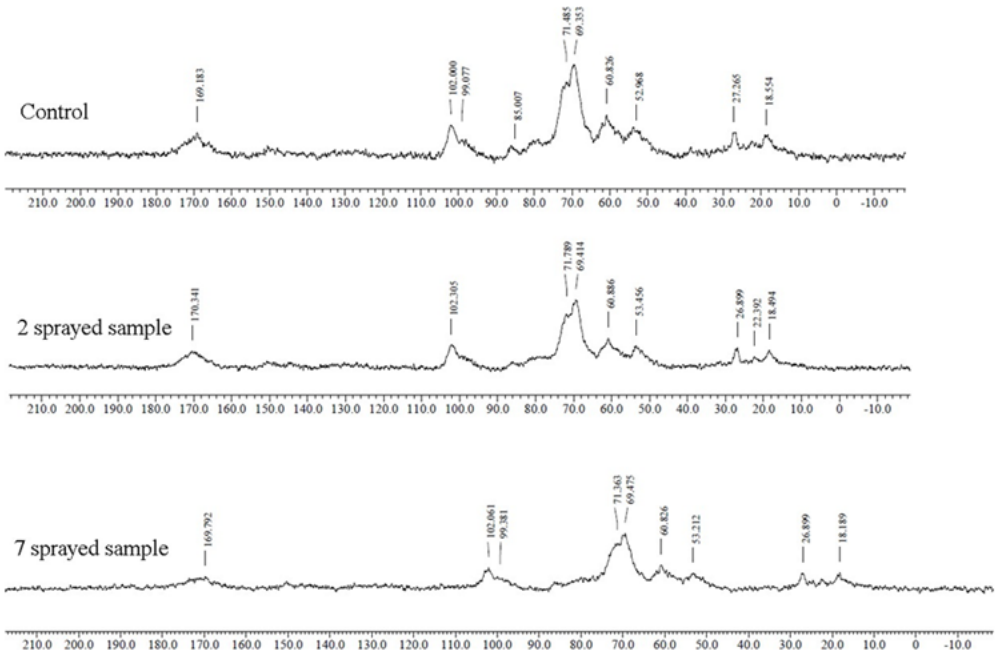

Figure 39: 13C Solid state NMR – Coriander.

Control	2 sprayed	7 sprayed	Typical Assignment
169.1	170.3	170	C=O (acids, esters)
102.0, shoulder at 99	102.0 (asymmetric)	102.0 (asymmetric)	C=C (alkene)
85 (possible spinning sideband)	85 (possible spinning sideband)	85 (possible spinning sideband)	-
~80 (possible spinning sideband)	~80 (possible spinning sideband)	~80 (possible spinning sideband)	-
71.4, 69.3 (overlapping peaks highest intensity)	71.4, 69.3 (overlapping peaks highest intensity)	71.4, 69.3 (overlapping peaks highest intensity)	RCH2O-
60.8 (possible spinning sideband)	60.8 (possible spinning sideband)	60.8 (possible spinning sideband)	-
53 (possible spinning sideband)	53 (possible spinning sideband)	53 (possible spinning sideband)	-
27.3	-	-	CH3CO-, R3CH
-	26.9	26.9	CH3CO-, R3CH
	22.4	-	CH3CO-
18.5	18.5	18.1	R2CH2

Table 18: C-13 Shifts (ppm) of Coriander.

The flavors of coriander come from fatty acids and volatile oils. The primary fatty acids present in coriander are linoleic and linolenic acids. The main essential oils are camphor, cyclohexanol acetate, limonene, and α-pinene. Numerous other substances have been reported such as the cyclic ether 1,8-cineol, eugenol, and geranyl acetate

- **Control:** shows peaks that are typical of C=O (acids), C=C, RCH2O-, CH3CO-, R3CH, and R2CH2 functional groups. These NMR peaks are consistent with the chemical compositions reported for coriander as described below.
- **2 sprayed sample:** The additional NMR peaks at 26.9 ppm and 22.4 ppm from the CR2 sample relative to the control might be due to increased concentrations of essential oils and/or fatty acids which leads to the increased taste, aroma, and hotness.
- **7 sprayed sample:** The lack of an apparent resonance at ~27 ppm and apparent resonances at 26.9 and 22.3 ppm might be correlated with the complete loss of taste, aroma, and hotness.

Cardamom

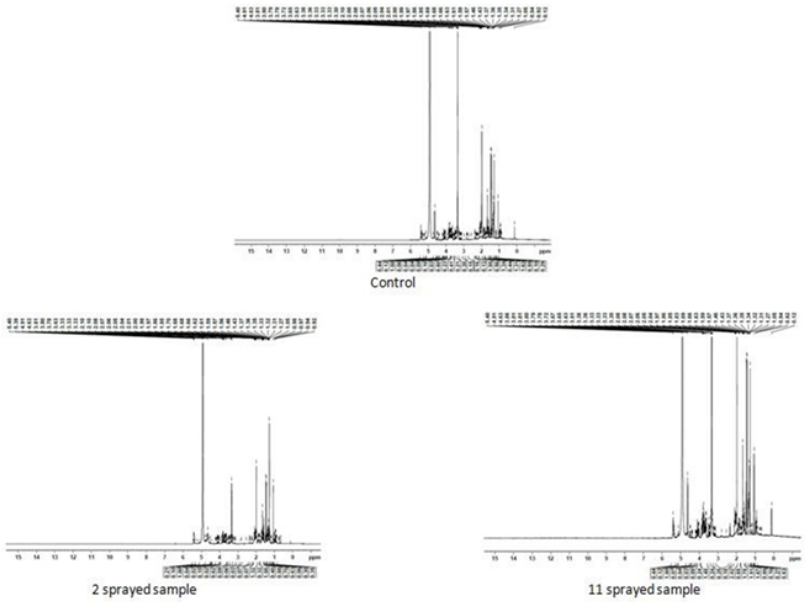

Figure 40: 1H-NMR – Cardamom.

&5.4 (m, 1H), 5.1 (t, 1H), 4.6 (s, 1H), 4.5 (d, 1H), 4.4 (q, 1H), 4.2 (q, 1H), 4.1 (d, 1H), 4.04 (m, 1H), 2.3 (m, 3H), 2.1 (m, 1H), 1.9(s, 1H), 1.7 (m, 1H), 1.4(d , 2H), 1.3 (m, 2H), 1.0 (s, 3H),0.9 (m, 3H) The 1H NMR spectra of the "cardamom" reveals the presence of a three proton singlet at δ 2.2 for a CH3 group on an aromatic ring, two peaks each of three-proton intensity at δ 0.7 and 0.9 for CH3. It also showsCH2 group at δ 1.2. The CH3 group resonances are attributed to the different CH3 groups. The sharp peak at δ 4.9 is due to the solvent (MeOD) and the broad peak at about 3.5 is due to the water. In order to distinguish between the 3 subsamples, the peak integral of each samples were normalized. The number of CH3 (and CH3aromatic) groups is the same in all samples. Other peaks are also similar in all samples and the observed changes in the physical form of the samples are not explained by NMR analysis.

Chemical Shift (ppm)	Control		2 sprayed		11 sprayed		Peak assign.
	Peak Integral	Normalized Peak Integral	Peak Integral	Normalized Peak Integral	Peak Integral	Normalized Peak Integral	
0.7-1.1	0.95	2	0.71	2	0.9	2	CH3
1.1-1.5	3.88	8	2.58	8	4	8	CH2
1.5- 1.7	1.78	4	1.4	4	1.78	4	CH
2.0-2.8	2.95	6	1.8	6	2.85	6	CH3 ar
3.4-4.7	2.84	6	1.84	6	1.47	6	
5.3-5.4	0.44	1	0.31	1	0.44	1	CH=CH

Table 19: C-13 Shifts (ppm) of Cardamom.

TEM

Pepper:

Figure F41(a): HR-TEM electron diffraction pattern of pepper powder samples.

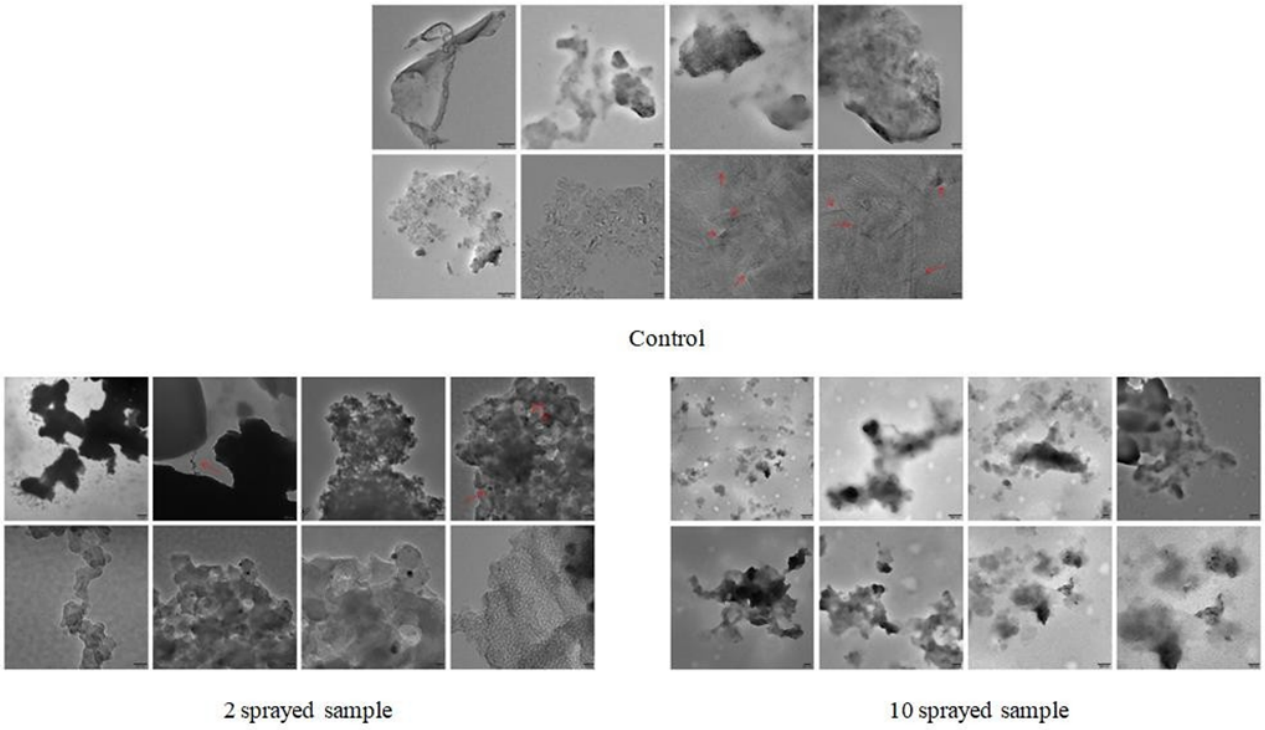

Figure 41(b): HR-TEM bright field images of pepper powder samples.

Further, the TEM images depicted in Figure 5 clearly demonstrates the structural changes,

Sl.No	HR-TEM	Control	2 sprayed	10 sprayed
1	Electron diffraction pattern	Two polycrystalline structure, (n)>>10 and static uniform	One poly crystalline present (n) <<10	Amorphous structure and spraying progressively decreasing the phases and of crystallites up to a non crystalline texture.
2	Bright field images	Different amorphous shaped fragments (<2μm) Crystallites also present.	Different amorphous shaped fragments (<1.5μm) Abundant dark spherical (10-20 nm diameter) nano particle seen. The crystallites sizes are lower than control.	Different amorphous shaped fragments (0.1-1.5μm) Non crystalline texture seen. Dark spherical nano particles are absent.

Table 20: TEM analysis of pepper powder samples.

Sprayings altered the degree of crystallinity and size of amorphous – shaped fragments.

Chili pepper:

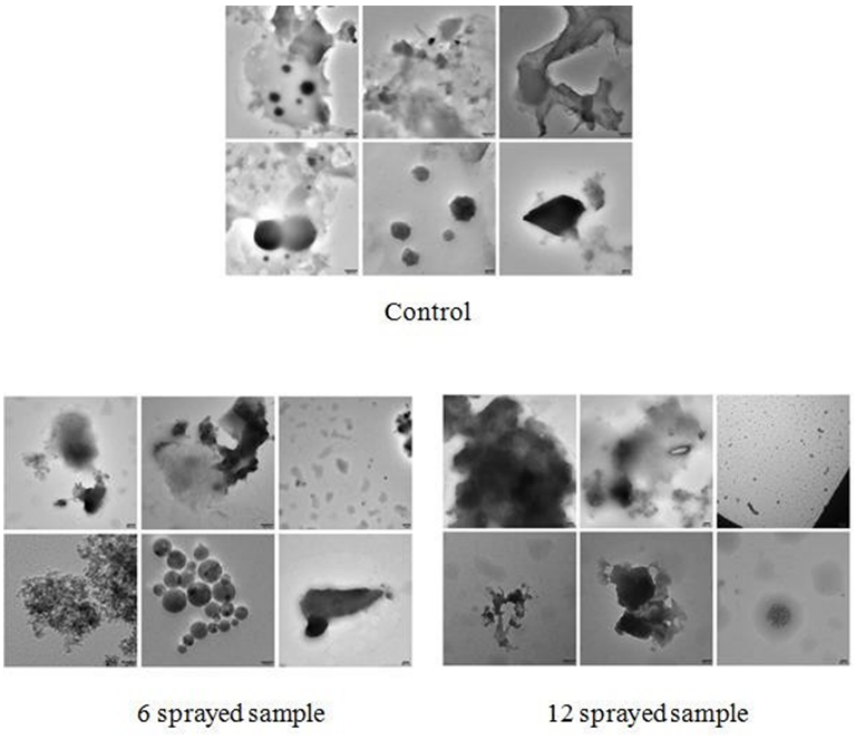

Figure 42: HR-TEM (Bright-field images) of Chili powder.

	Control	6 sprayed	12 sprayed
Particles and size	individual particles range 100 – 500 nm (spherical type) and 1 – 5 µm (polygonal type)	oblate ellipsoids (10 –20 nm), spherical (5 –50 nm) and droplet-like objects (0.5 – 2 µm)	Only droplet-like objects (0.5 – 1 µm) and part of them have inclusions (10-100 nm)
Shape	amorphous inclusions	separated clusters	semi-spherical

Table 21: TEM analysis of Chilli Pepper.

- **Control sample:** Average main sizes (Feret's diameter) of individual particles range 100 – 500 nm (spherical type) and 1 – 5 µm (polygonal type). In this sample, particles are observed either as inclusions in the amorphous fragments, and as individuals. Particle size does not seem to change significantly between these two cases.
- **6 Sprayed Sample:** Differently from the control, in the 6 sprayed sample spherical particles are not observed as inclusions of the amorphous fragments, but in separated clusters. Observed particles show three different combinations of aspect and shape. Nanosized particles are either oblate ellipsoids (bottom left) with narrow size range (10 – 20 nm), or spherical (bottom central) with larger size range (5 – 50 nm). Both types are observed as clusters. Polygonal particles size is instead comparable to the control sample. Moreover, droplet-like objects are observed, that are not detected in the control sample; these range 0.5 – 2 µm, show polygonal shape as well, and appear as spread over the sample surface.
- **12 Sprayed Sample:** Differently from the control and low treated samples, in the high treated sample individual particles are not observed, with the only exceeption of the droplet-like type. Size range of these is 0.5 – 1 µm, and the shape is semi-spherical. These features are different from those observed for the droplet-like type of the 6 sprayed sample, the latter having larger size range and non spherical shape. The enhanced image of one of these droplets show that at least part of them have inclusions, having the aspect of nanosized particulates with size range 10- 100 nm roughly.

Ginger:

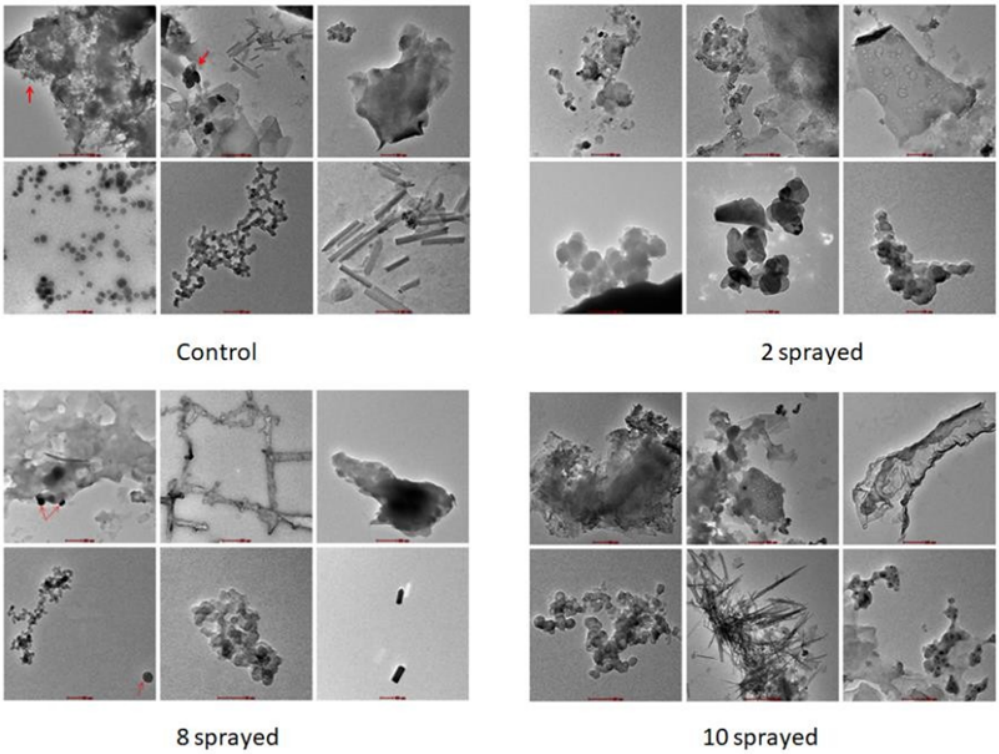

Figure 43: TEM Bright-field images of ginger powder samples.

- **Control:** Average main size of aggregates (1-3µm); fragments (0.5-1µm). Small particle size are individual particles (30-70nm) and chain – like clusters (30-40nm). Needle like particle's length and width are 50-250 nm and 10-30 nm (ratio 3-8 average 6). Nano sized (regular circular contour) and submicron particles show peculiar features associated to the clustering shape and/or to particle shape.
- **2 Sprayed Sample:** Needle like and nano size particles are absent. Average main size of aggregate particles (0.5-2µm); fragments (0.2-0.8µm) (became smaller than control) and clustered particles (60-70nm). The clusters of nano sized particles (contour in wavy) are larger than control and clustering shape appears more nest like than chain like. Sponge like fragments is clearly distinguishable from other fragments.
- **8 Sprayed Sample:** Needle like and individual nano sized particles are absent. Chalk like and fiber shaped structures seen. Average main size of amorphous fragment (0.5-2µm); fibre (0.3-0.5 µm length). The fibers showed an organized reciprocal orientation described by angles up to 90 degree between fiber extremities. In small particles; clustered (20-40nm); semispherical (70- 100nm).
- **10 Sprayed Sample:** Needle like particles again observed lower size and clustering features differ from control. Nano sized particles appear in clusters not individual as in control. Submicron particles are absent. The size of aggregate (0.5-2µm), fragment (0.51µm), cluster (20-30 nm) and clusters show an intermediate shape chain and nest like in control and 2 sprayed respectively. Needle like particles length and width are 0.5-2µm and 20-30nm (far higher than control 25-70nm). Individual needle like particles are sporadic (in control individual and small cluster) but most of them are grouped in large and crowded cluster and contrary to control preferential orientation is not observed but sponge like large particles present.

Curry Leaves: The 3 sprayed causes rearrangement of atoms in a polycrystalline texture, but this concerns only a minor portion of the overall sample. The 9 spraying, causes a general rearrangement of the atomic structure of the sample, leading to a significant crystalline texture, that is, almost completely different from the texture of the control.

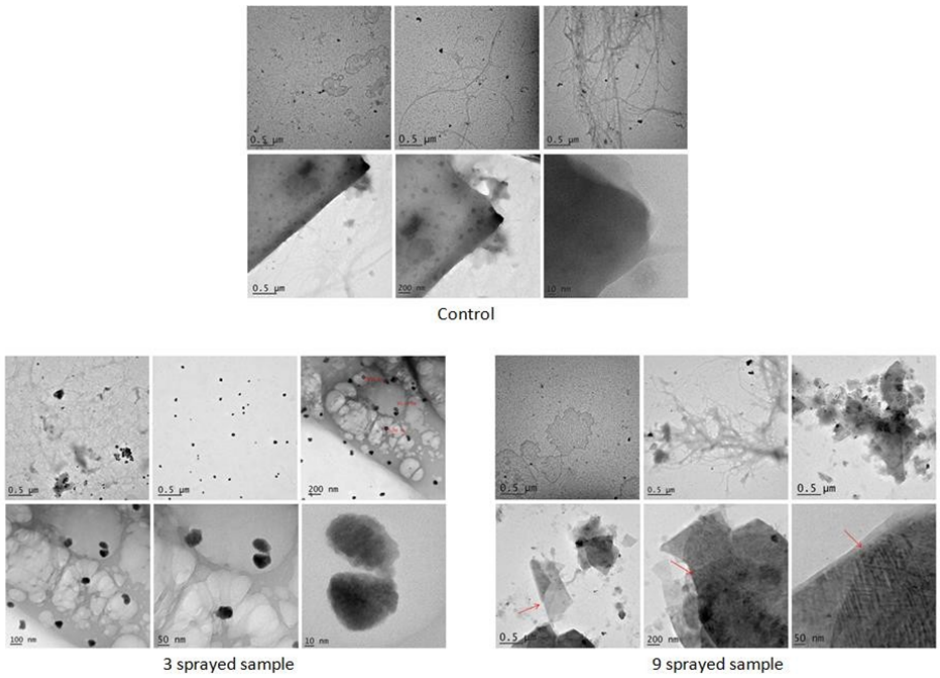

Figure 44: TEM Bright-field images of curry leaves powder samples.

Sl.No	Parameters	Control	3 sprayed	9 sprayed
1	Electron diffraction pattern	Amorphous	Polycrystalline and number is 2-10. One single circular perimeter seen. Interplanery distance is 0.20nm	Polycrystalline and number is 2-10. Three circular concentric perimeter and the fourth one is only weakly distinguishable. Interplanery distance is 0.54, 0.31, 0.18 and 0.16nm. (Increasing number of spraying altered the atoms arrangement and difference is very clear)
2	Bright field images	Semicircular or elongated (0.1-1µm); single or clustered fibre (perimeter range 1-5µm for single); and evenly distributed. Dark nano particles (10-30nm) seen. Non crystalline texture.	As control same matrix components seen but with different size and morphology. Unevenly distributed fibres appears as clusters. no particles appear single or in clusters (20-80nm). Texture is altered and minor crystalline behavior appeared.	Smooth surface is similar to control (0.1 - 1µm diameter). Dark nano particles 10-30 nm evenly distributed, one crystalline compound and bending contour are evident. Crystallites have preferential orientation.

Table 22: TEM analysis of curry leaves powder.

Fenugreek:

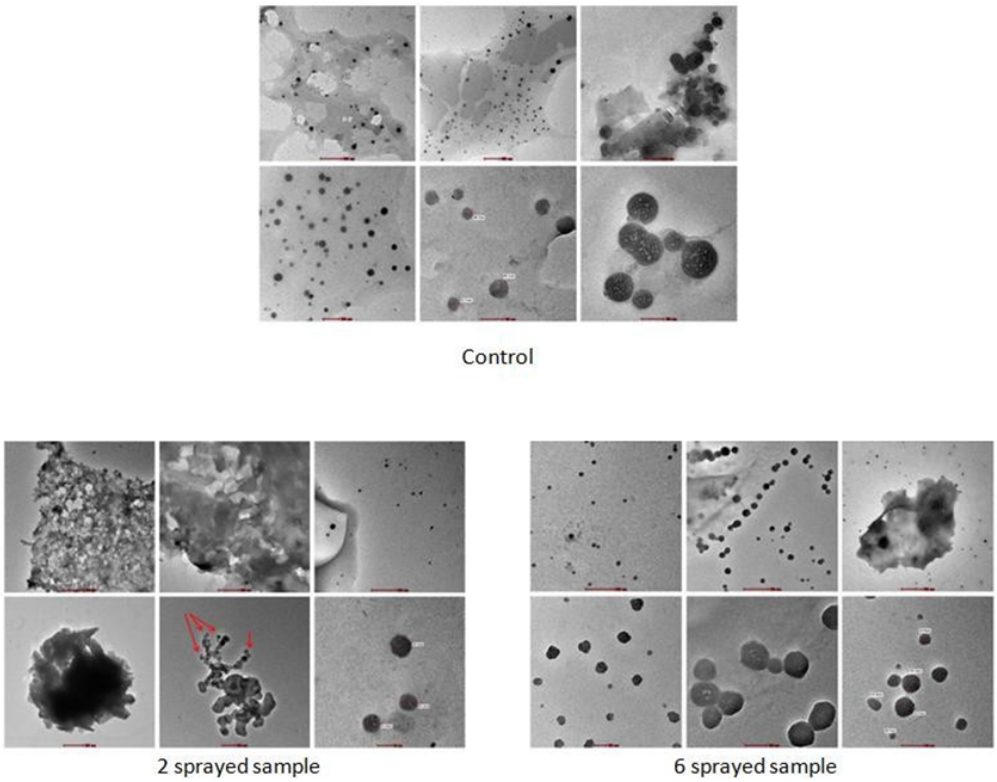

Figure 45: TEM Bright-field images of Fenugreek samples.

With respect to the control, 2and 6 sprayings affect the original sample matrix, and each spraying affects it differently. 2 spraying causes a general decrease of the nanosized particle fraction, and the loss of the ultrafine fraction; also, particles spatial arrangement is different from control , since particle clusters are observed, while in the control particles are observed almost only individually. It is anyway possible that the apparent decrease of the nanosized particle fraction in the 2 sprayed sample is, instead, the result of a more significant clustering arrangement that affects the number of individual particles. The 6 sprayed sample, instead, causes minor changes concerning the abundance of ultrafine and nanosized particles, with respect to control. However, major changes concern both the spatial arrangement of particles (alignments) and the distribution of mass within particle. Significant differences are also observed in the aggregates. With respect to control, due to both 2 and 6 sprayings, aggregates appear more dense, that is containing more abundant mass, while the distribution of mass within aggregate remain uneven, although the degree of non-homogeneity decrease from 2 to 6 sprayings.

Cumin: With respect to the control, 2 spraying seems to affect the sample matrix mildly, since all features concerning the matrix components, dimensional ranges, morphology of particulates, relative abundances of components, and spatial arrangements are maintained similar to those of the control, with the only exception of the morphology (and distribution of mass) of the "spherical shape" type of aggregate. Differently, 6 spraying affects the sample more significantly. This concerns both aggregate types and small particles. In the first case, only one of the two types identified in the control and 2 sprayed sample is observed in 6 sprayed sample, and with evident differences of aspect/morphology; in the second case, small particles show higher numerosity, narrower size range, and partially different spatial arrangement, with respect to control and 2 sprayed samples.

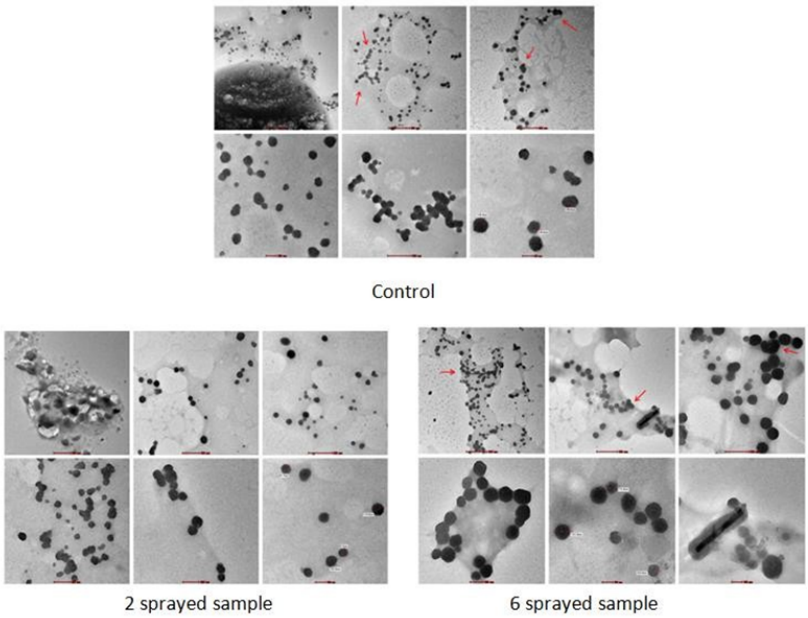

Figure 46: TEM Bright-field images of Cumin samples.

Black Cumin:

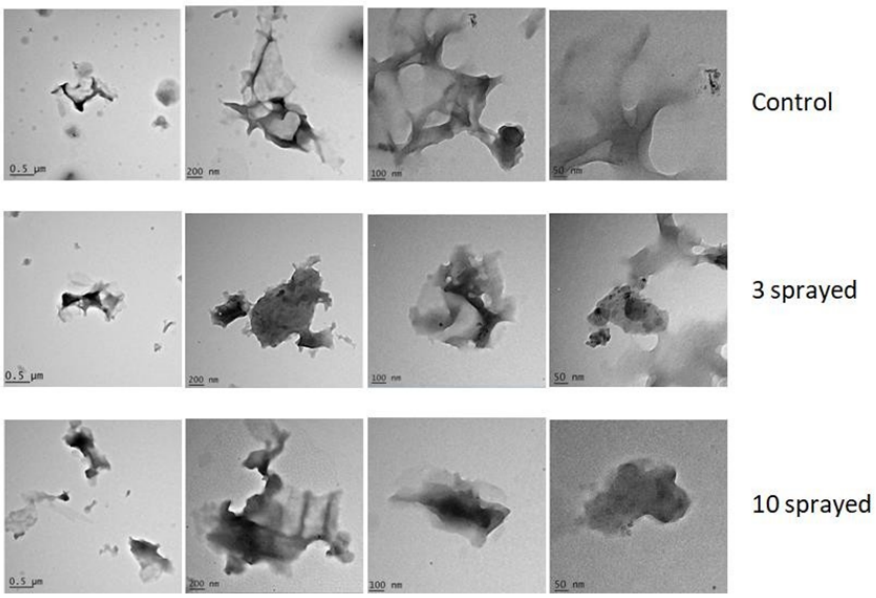

Figure 47: TEM Bright-field images of Black cumin samples.

- **Control:** The particles are amorphous with less than 500 nm size. There are smaller particle with less than 50 nm size as well. White particles appear black in the images due to their relatively high electron density.

- **3 Sprayed Sample:** The images are more or less similar to the control sample. Particles are amorphous with maximum 500 nm size. However, the images at higher magnification show very small white dots (20 nm or so, but round shape) attached to the bigger particles. The bigger particles are coated with these small particles therefore, the general bitterness is reduced.

The white area indicates the presence of low thickness particles generated due to the spraying. These very small particles are more crystalline than the original big particles.

- **10 sprayed sample:** The images are more or less similar to the control sample. Particles are amorphous with maximum 500 nm size. The small particles observed in 3 sprayed sample are disappeared in 11 sprayed sample due to further spraying. Therefore, the aroma is reduced. There is no coating on the particles compared to the previous 2 samples, therefore, the particles are very bitter and palatable.

- **Electron Diffraction Patterns**

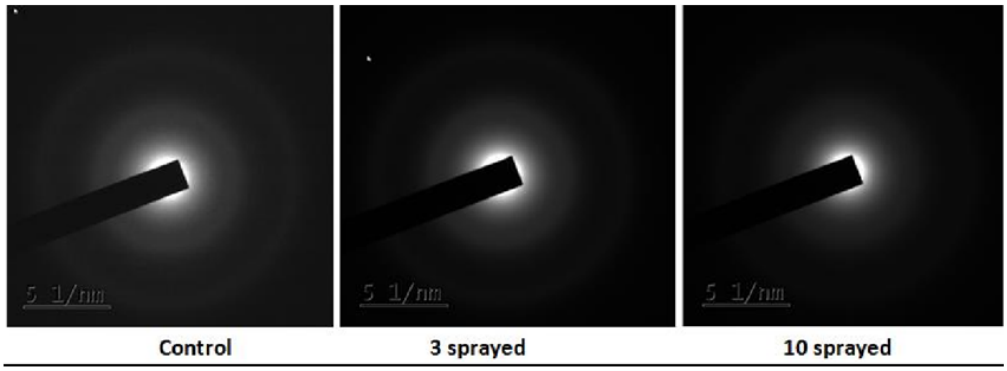

Figure 48: Electron diffraction patterns of Black cumin samples.

No clear differences is observed between the patterns of the samples. This suggests similar texture and crystalline structure for all samples.

The TEM analysis suggest that the control sample has amorphous shape, however, small crystalline particles are appearing upon 3 spraying (increasing the taste and aroma). These small particles are coated on the big particles. These coating are removed upon 10 sprayings, results in decreasing the taste.

Coriander:

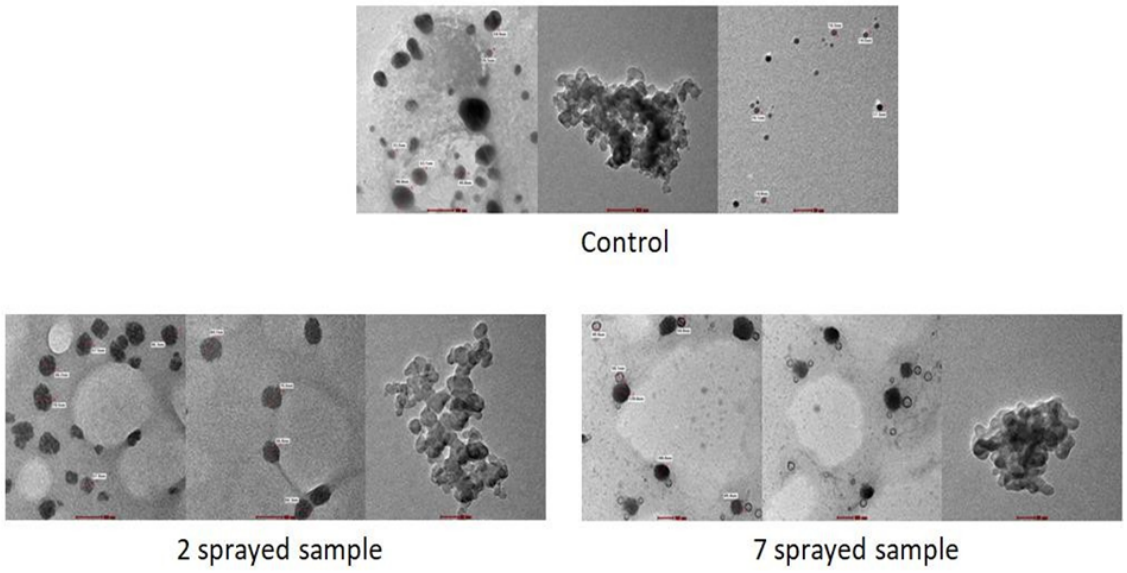

Figure 49: TEM Bright-field images of Corainder samples.

A plot showing the apparent particle size range is given below.

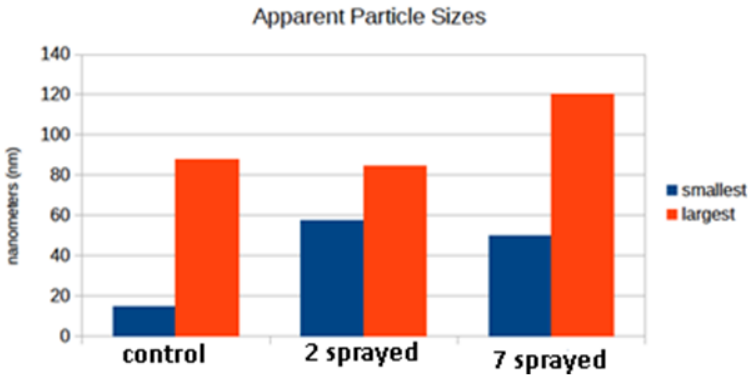

Figure 50: TEM particle size range of Corainder samples.

The energy dispersive x-ray (EDX)spectroscopy data of each sample is provided below.

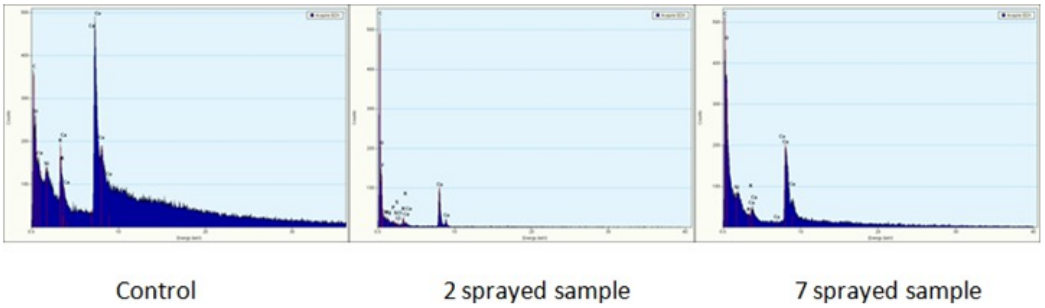

Figure 51: EDX spectra of Corainder samples.

Control	2 sprayed	7 sprayed
Particles: show individual rounded particle 14.5 to 88 nm, present agglomerated.	Particles: show individual rounded 57.5 to 84.7 nm, present agglomerated.	Particles: show both individual rounded particles and agglomeration of these rounded particle, but agglomeration is lesser degree but with greater density. 49.9 nm size particles are ring-like structure. The larger particle (100nm-120nm) are dense similar to the control particle.
Contains: organic compounds seen as fatty acids, volatile oil, CHO, etc. Also C, O2, Cu, Si, K, Ca, Co	Contains: C, O2, Fl, Mg, K, S, Cl, Ca, Cu. Also linolenic acid, camphor, cyclohexanol acetate. The changes in the particles size might be related to the change in the hotness.	Contains: C,O2, Si, K, Ca, Co, Cu. The ring like structure may be related to the difference in the profile compared to control and 2 sprayed samples.
Contains: organic compounds seen as fatty acids, volatile oil, CHO, etc. Also C, O2, Cu, Si, K, Ca, Co	Contains: C, O2, Fl, Mg, K, S, Cl, Ca, Cu. Also linolenic acid, camphor, cyclohexanol acetate. The changes in the particles size might be related to the change in the hotness.	Contains: C,O2, Si, K, Ca, Co, Cu. The ring like structure may be related to the difference in the profile compared to control and 2 sprayed samples.

Table 23: TEM analysis of Coriander samples.

Cardamom: The TEM analysis suggest that the structure of the sample has been broken upon spraying. The 2 sprayed sample which is easily dissolvable shows a clear different response in the TEM analysis. While 11 sprayed sample TEM images are more or less similar to the control sample, there are evidence of very small particles (generated due to the spraying). The aroma and taste of the sample follows the TEM response.

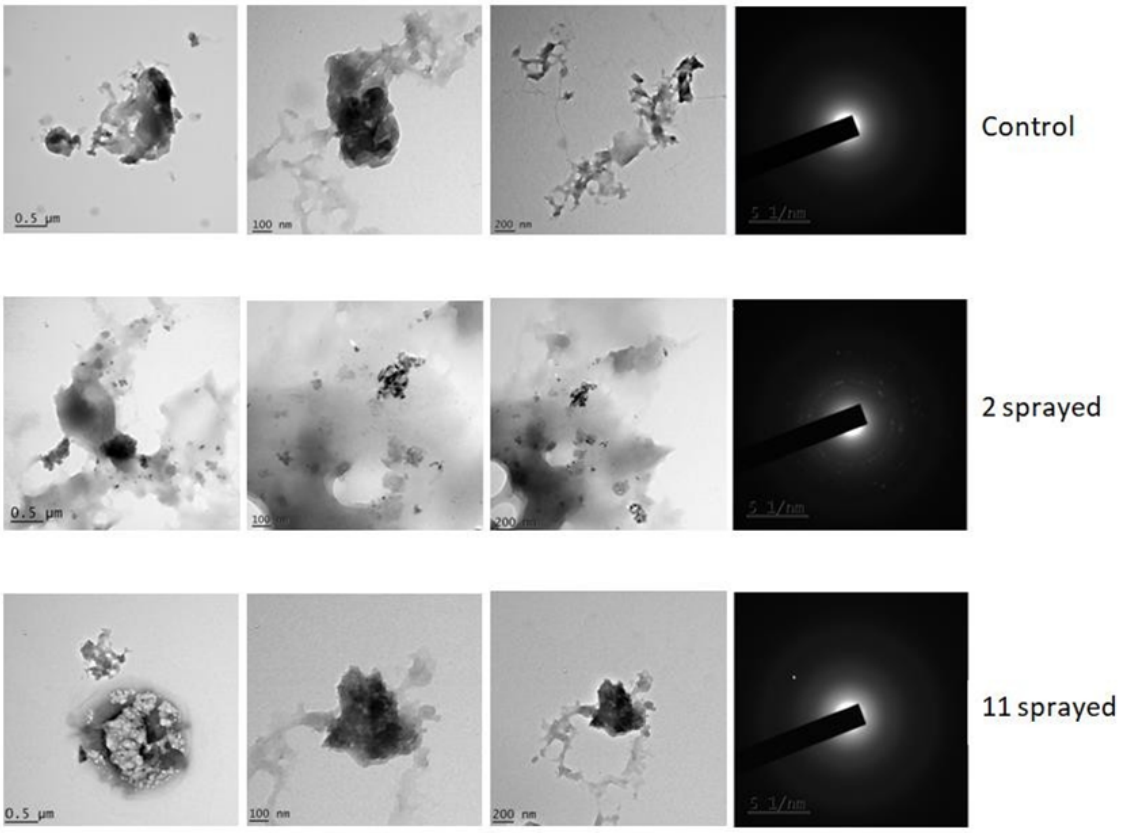

Figure 52: TEM Bright-field images of Cardamom samples.

S.no	Parameter	Control	2 sprayed	11 sprayed
1	Particle size and shape	Average 1 micron small particles 200nm, and amorphous.	Particles much smaller and appear in big aggregates (50 nm to a few microns). Small particles are round shaped and amorphous and aggregates.	Average 1 micron to 200nm, round and amorphous shape and low thickness (about 200nm)

Table 24: TEM analysis of Cardamom samples.

3D Fluorescence Spectroscopy

Pepper: All the samples are fluorescence active. There is more electron density in contour region in the fluorescence diagram of 10 sprayed than sample 2 sprayed and control. In 2 sprayed and 10 sprayed samples changing the excitation wavelength from 250nm to 500nm the emission occurs in the range of 400nm to 550nm only. But in case of control sample excitation in this range gives emission below 500nm. In 10 sprayed however there is the appearance of new peak in the range of 630nm to 650nm which is not present in control and 2 sprayed. The decrease in the hotness and aroma of 10 sprayed sample upon spraying may be because of the transform of the piperine into isochavici which is a tasteless molecule.

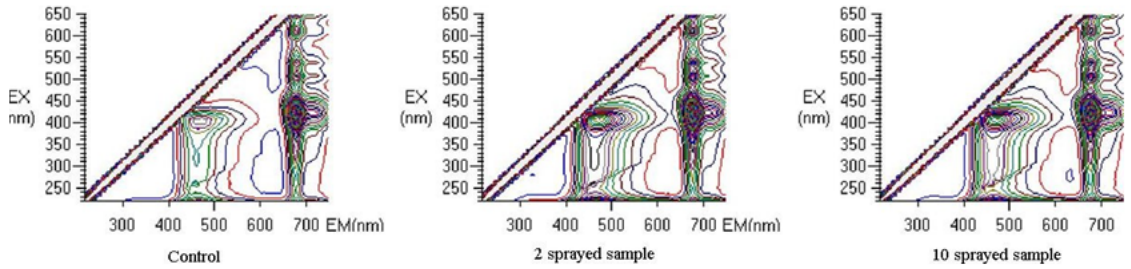

Figure 53: 3D Fluorescence spectra of Pepper.

Chili Pepper

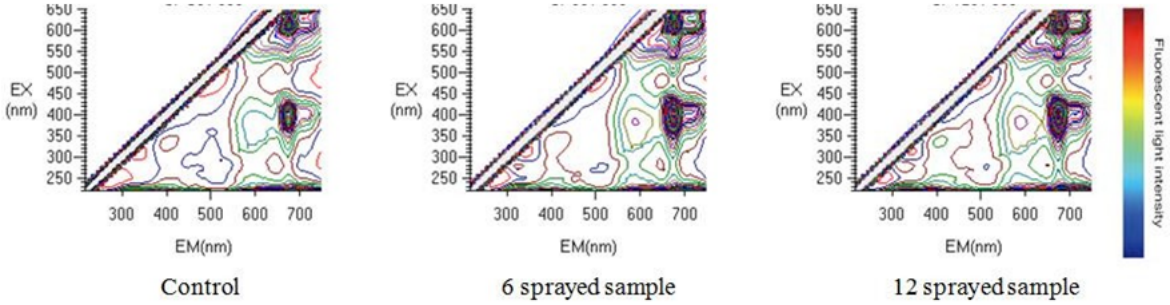

Figure 54: 3D Fluorescence spectra of Chili powder.

The increase and the decrease in the hotness as compared to the control has a profound effect on the island contours. Specifically, the island contour gets bigger (top island) and longer (bottom island) when the hotness changed. However, the center of the island contour did not change. The lower energy emission bands (Em = 700 nm and higher) of the 6 and 12 sprayed samples become more pronounced. The changes in the dimension of island contours can be interpreted as increased response/ emission of the sample from the excitation. Physically, this is a result of increased number of electrons transitioning from the higher energy to lower energy state. Aside from this, the appearance of the lower energy emission bands can be thought to be from the improved density of states. Alteration on the hotness content appeared to modify the fluorescence fingerprint of chili powder.